5-2009

Inducing a Normal Phenotype in Breast Epithelial Cells Using a Three-Dimensional Basement Membrane Extract Culture System: A Study on the Reversion of Cancer

Ross H. Booth
Utah State University

INDUCING A NORMAL PHENOTYPE IN BREAST EPITHELIAL CELLS USING A THREE-DIMENSIONAL BASEMENT MEMBRANE EXTRACT CULTURE SYSTEM: A STUDY ON THE REVERSION OF CANCER

by

Ross H. Booth

A thesis submitted in partial fulfillment
of the requirements for the degree

of

MASTER OF SCIENCE

In

Biological Engineering

Approved:

_____	_____
Dr. Soonjo Kwon	Dr. Timothy Doyle
Major Professor	Committee Member
_____	_____
Dr. David Britt	Dr. Byron Burnham
Committee Member	Dean of Graduate Studies

UTAH STATE UNIVERSITY
Logan, Utah

2009

ABSTRACT

Inducing a Normal Phenotype in Breast Epithelial Cells Using a Three-Dimensional Basement Membrane Extract Culture System:

A Study on the Reversion of Cancer

by

Ross H. Booth, Master of Science

Utah State University, 2009

Major Professor: Dr. Soonjo Kwon
Department: Biological and Irrigation Engineering

Experimentally, traditional developmental models and transgenic animals consistently underscore the importance of studying cell behavior in the correct tissue context. However, live animal experimentation is inherently complex, and systematic assessment of the effects of individual variables, such as cell shape and matrix compliance on cell behavior, is extremely difficult at best. Two-dimensional monolayer culture of key individual cell types has provided abundant, fundamental information on cell response, but cannot be used to show the normal phenotype of breast epithelial cells. Furthermore, their results often fail to translate into *in vivo* and clinical studies. It has been previously established that normal human breast epithelial cells can form their original phenotype as seen *in vivo* when embedded in or layered on reconstituted basement membrane extract. This phenotype is characterized as a single or double layer of polarized cells in acinar form

with a lumen devoid of cells. Most malignant cell lines cultured under the same conditions exhibit severe morphological deformities, including colony overgrowth, luminal filling (hyperplasia), and resistance to apoptosis. It was hypothesized that malignant breast cells can be reverted to a normal phenotype through the manipulation of two factors: control of the environment via extra-cellular matrix proteins, and control of cellular pathways via signaling inhibitors. It was observed that high levels of epidermal growth factor resulted in disrupted multi-acinar formations. Inhibition of the protein complex known as mammalian target of rapamycin is currently being investigated as a potential method for cancer treatment. Exposure of rapamycin, mammalian target of rapamycin's primary inhibitor, led to decreased proliferation and increased caspase activity. Through the exposure to rapamycin in three-dimensional cultures, proliferation was reduced in malignant cells, while normal cells were not significantly affected. Unfixed fluorescent staining with ethidium bromide indicated the presence of luminal cell death. Increased structural organization was observed by immunofluorescent staining of F-actin and β-catenin. Through RT-PCR analysis, increased expression of a number of genes related to polarity and structural organization was detected in malignant cells exposed to rapamycin. Further study will be required to better characterize the reversion effects of rapamycin and its derivatives.

(74 pages)

DEDICATION

This thesis is dedicated to my amazing and brilliant parents Ray and Dawna. You have given me all your help and support through everything I have done in my life. You have been with me through the good times, the bad times, the easy times, and the hard times. I would certainly not have been able to accomplish what I have without you pushing me to always do my best. For all of this and so much more, thank you. And to my wife, Stella, for staying supportive and putting up with all my late nights at the lab. I love you all!

ACKNOWLEDGMENTS

I wish to express sincere appreciation to Dr. Soonjo Kwon for his guidance and all his help from start to finish, and to Drs. David Britt and Timothy Doyle for their assistance as members of the advisory committee. In addition, thanks to those who gave their time to help me with my research, including my advisory committee, Ninglin Yin, Giovanni Rompato, Joe Shope, and Eric Monson. Special thanks to the other members of the lab, especially Hemang Patel, who have helped me immensely over the past two years. Also, thank you to the BIE department, and to the National Institutes of Health, who has kindly provided the grant through which our funding was possible.

Ross H. Booth

PREFACE

- Note that the term malignant is used frequently in this paper. The term “malignant” is often used to describe tumors that have ceased to be benign and have become invasive. In this paper (and much of the cited literature) the term malignant is intended to refer to all cancer cells.

CONTENTS

LIST OF TABLES

LIST OF FIGURES

LIST OF ABREVIATIONS

2D 2-Dimensional
3D 3-Dimensional
BCT.....Breast-Conserving Therapy
BM ..... Basement Membrane
ECM.....Extra-Cellular Matrix
EGF ..... Epidermal Growth Factor
EGFR ..... Epidermal Growth Factor Receptor
EHS.....Engelbreth-Holm Swarm
EMT ..... Epithelial-Mesenchymal Transition
FBS ..... Fetal Bovine Serum
LEP ..... Luminal Epithelial
MAPK.....Mitogen-Activated Protein Kinase
MEP ..... MyoEPithelial
MEGM.....Mammary Epithelial Growth Medium
MMP ..... Matrix MetalloProteinase
mTOR ..... mammalian Target Of Rapamycin
HBE.....Human Breast Epithelial
PI3 .....Phosphatidylinositol-3-OH
rBME ..... reconstituted Basement Membrane Extract
RT-PCR .....Reverse Transcriptase Polymerase Chain Reaction
SMT .....Somatic Mutation Theory
VEGF.....Vascular Endothelial Growth Factor

CHAPTER 1

INTRODUCTION

The history of cancer research, as young as it is, has gone through rapid changes in a short period of time. As new causes for cancer have been discovered throughout the 20th century - from the Rous Sarcoma Virus in 1910 to the first proto-oncogene in 1975 and the now hundreds of suspect carcinogens being rigorously investigated – the focus of cancer researchers has constantly been changing direction. As cancer ascends to become the world's leading cause of death, the fierce debate over where researchers should focus their attention continues. While most traditional studies of cancer focus primarily on the signaling, chemistry, and genetics of individual cancer cells, a growing movement of researchers has been publishing work asserting that tissue microenvironmental influences should be held coequal. For many, adopting this perspective has required them to take a unique approach to cancer research, but history has shown that exploring new paths of inquiry can be productive to scientific progress.

1.1 Achieving Physiological Accuracy in Cellular Models

The case for the importance of cell-based *in vitro* models needs little persuasion. Before clinical studies can begin, the concept in question must be well established in laboratory studies. While animal models can be very useful, *in vitro* models are often preferred due to ethical, technical, and financial constraints. In addition, a greater amount of experimental control is allotted to the researcher using cell-based models. For this reason there has been a very high demand for effective cell-based models in cancer research [1].

However, for a cellular model to be useful, it must properly represent conditions found *in vivo*. One of the advantages of human cell-based models over animal studies is that the researcher can avoid complications from species-dependent concepts. There remains an advantage for animal models in that they address a higher level of complexity which existing cellular models do not have. This level of complexity must be addressed in cellular models to overcome this advantage.

1.1.1 Adding an Extra Dimension

Cytotoxic agents and tumor suppressors tested successfully on two-Dimensional (2D) plastic cultures often fail to translate successfully into *in vivo* research. This resistance to signaling factors is also sometimes present in three-dimensional (3D) culture systems [2]. This presents a real issue for 2D cultures, as they fail to address this resistance to drugs which is often present in actual tissues.

Accurate cell differentiation and functionality often has 3D spatial requirements [3], and the polarized phenotype that epithelial cells possess *in vivo* is rarely observed in 2D cultures. Breast cancers are subdivided into at least 18 distinct subtypes [4], each with unique histological properties. These can be difficult to differentiate visually from appearance on a plastic monolayer, but these differences are better visually recognized when placed in 3D culture models (**Figure 1)**. Even the differences between normal and cancer cells can be difficult to distinguish in 2D, while easily characterized when placed in 3D cultures.

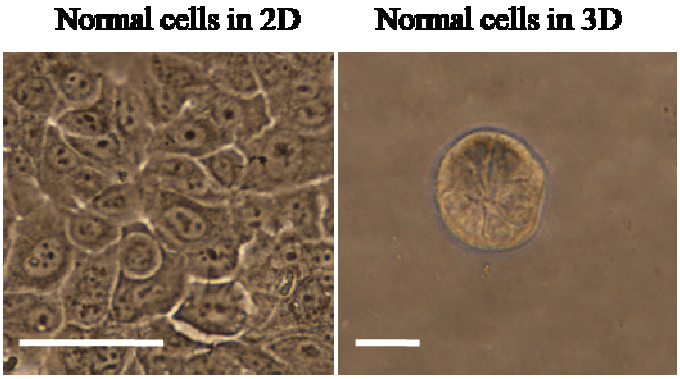

Figure 1: Normal Cells Cultured in 2D and 3D on Day 6 of Culture
The difference between morphologies of cells cultured in 2D and 3D are clear. Monolayer cultures adhere to the plastic surface and reach confluence, while the same cells cultured in 3D will spread 3-dimensionally and limit their growth. (scale bars = 25 µm)

1.1.2 Experimental Control

There is an inverse correlation between model complexity and experimental control. Therefore, a balance must be found between maximizing model complexity and maintaining control over experimental design. To simplify, controllable factors have been lumped into two classes: signal molecules and microenvironment. The importance of the microenvironment has often been understated as excitement over the discovery of oncogenes has led researchers to focus their attention on genetic mutation as the cause of cancer and metastasis. However, data contradictory to the somatic mutation theory [5] has allowed new theories to be proposed. These theories suggest that research should be looking not only for intracellular targets, but also at the interactions between cancer cells and their microenvironment.

The microenvironment includes the 3D arrangement of the cells themselves, as well as the surrounding extra-cellular matrix (ECM). The ECM is not merely a structural

scaffold, but directly affects a series of intracellular pathways which modify the expressed phenotype in a variety of ways [6]. A reciprocal interaction between tissue architecture and gene expression is strongly supported [7] and will be discussed in the following section.

1.1.3 Mechanisms of Microenvironmental Impact on Phenotype

Two broad hypotheses were proposed in a recent review article which effectively asserts the importance of the microenvironment in cancer development.

> First, that tumour cells with abnormal genomes should be capable of becoming phenotypically normal if their normal microenvironment can be restored, and, secondly (and conversely), that the destruction of tissue structure itself could be an oncogenic event, even in the absence of initial genetic mutation. [8]

Indeed, bolder advocates of the 3D method suggest that tissues are constantly being bombarded with oncogenic factors, and that the proper maintenance of tissue architecture and polarity is a sole factor preventing oncogenesis [3, 9]. There are two general methods through which the ECM directs cell pathways. The first is directly through membrane-bound receptors on the exterior cells, and the second is through other pathways which are indirectly dependent on morphology [10]. The mechanisms through which epithelial cells receive cues from the surrounding ECM have been studied extensively. The most well established mechanism is through membrane-bound integrins [11].

Cells in a dynamic human body are constantly undergoing physical forces. These forces include shear stress, compression and tension forces, and hydrostatic pressure. Cells have mechanisms for detecting these forces, and they can have a major effect on cellular pathology, including cancer. The loss of tensional homeostasis can increase cancer risks and compromise treatment [12, 13]. Culturing in 3D is associated with an increase in global

histone acetylation [14], which results in chromatin condensation and a decrease in cell proliferation.

Matrix metallo-proteinases (MMPs) are ECM-degrading proteins which are often dispatched into the stroma [15]. Epithelial mesenchymal transition (EMT), a phenotypic alteration in which epithelial cells detach from their neighbors and the underlying basement membrane and become more motile and migratory, which has profound effects on tumor metastasis, is known to be induced by pathways including MMPs. However, this process has been shown to be limited by changes in cell shape [16]. Another recent study measuring the branching locations of metastasizing cells using micropatterning found that, remarkably, branch sites were located only on tubule corners [8], indicating a dependency on tissue architecture.

1.1.4 The Functional Unit

One primary difference between 3D and 2D culture models is the functional unit. Traditionally the functional unit was the individual cell, but in 3D cultures the functional unit is the entire structure the cells form [17]. As a result, a greater amount of criteria can be investigated on a single functional unit which couldn't before, such as tissue polarity, cell-cell communication, multicellular structure, and localization of function.

Identification of the functional unit is a first step in experimental design. In the case of breast cancer, the mammary acinus is the unit of interest, and is characterized by a spherical formation consisting of a single layer of epithelial cells surrounding an empty lumen. The purpose of the lumen in ducts is to carry milk proteins to the branching

locations and ultimately the nipple. The development of ducts from alveoli is led by a complex differentiation process which is still poorly understood [18]. The process of alveolar branching and the generation of ducts has been observed to be dependent upon communication with the ECM surroundings [19]. These cells go through differentiation many times through the life of the individual, including periods such as puberty and lactation. Perhaps this is why the breast is so vulnerable to cancer.

In most cell lines, the structure forms from a single cell over a period of 6-10 days (**Figure 2)** in 3D culture. The precise mechanisms are not well understood, but the cells begin to polarize, leading to survival of outer cells, and death of luminal cells.

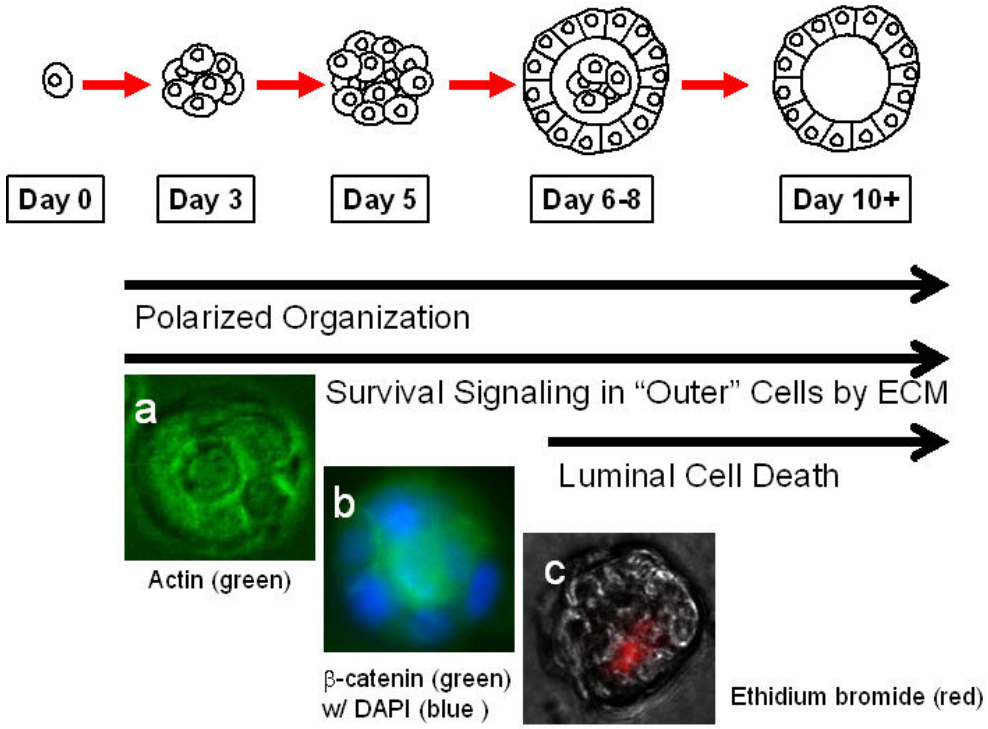

Figure 2: Formation of the Mammary Gland Acinus *in vitro*
The functional unit for human breast epithelial cells is a spherical acinus consisting of an outer layer of cells and a lumen devoid of cells. In culture, polarization of the outer cells leads to apoptosis of un-polarized cells in the center [9].

1.1.5 ECM and Basolateral Polarity

A unique characteristic of epithelial cells is their ability to functionally polarize. The membrane-bound proteins and biochemical activity on each (basal and luminal) side are different in polarized cells. For example, in the breast acinus, the activity on the luminal side includes cues which incite apoptosis on interior cells, and the activity on the basal side includes interaction with the basement membrane. Myoepithelial cells, while normally present *in vivo*, are normally left out of these cultures. This is because their functional role in polarity appears to be maintenance of the basement membrane [20]. Luminal formation is still poorly understood, but is mostly likely caused by induced apoptosis of interior cells separated from the exterior layer. As this only happens in the presence of a polarized outer layer, a signal is likely being transmitted from the luminal edge of the exterior cells which is initiating terminal pathways [21].

As early as the 1970s, the importance of the basement membrane and basolateral polarity in structural development of healthy tissues was being discussed [22], and normal polarity was achieved using ECM-based gels in culture as early as 1992 [23]. Choice of ECM is not only important because it provides physical support and special freedom for acinar formation; it promotes cell polarity. However, basal cells are only responsive to the correct ECM recipe. While collagen is the most commonly found ECM protein in the body and is commonly used in tissue engineering, polarity has been found to be preserved best when using proteins which closely resemble the basement membrane [24]. The mixture derived commercially from the Engelbroth-Holm Swarm (EHS) tumor, better known as

reconstituted basement membrane extract (rBME), was found experimentally to be the best option and is still used today.

The primary component in rBME is laminin-I, which has been found to directly induce higher integrin activity and better adhesion in preadipocyte cells [25]. Laminin-I is also known to be have a strong role in early tissue organization of embryos in the womb [26]. Other components of rBME include procollagen IV, heparin sulfate proteoglycan, and entactin [27]. It is likely that all these basement membrane components play a role in directing an optimal phenotype, though these roles are still not well characterized. Still, laminin is believed to be the most important component [28].

1.2 Previous Studies

Table 1 lists several signal molecules which have been investigated using 3D culture models. *In vivo*, tumor cells lose some or all of their morphological organization in healthy tissue. Using 3D cultures as introduced in the previous section, cancer cells can be studied through morphological observation. In 2D, normal and malignant cells similarly form adherent monolayers, but when placed in 3D rBME, the difference becomes clear. Morphological disruptions are present in the malignant cultures just as they are *in vivo*. Through the manipulation of signal molecules, malignant cultures can be reverted back to a normal phenotype. This is commonly termed a reversion strategy.

Table 1: Previous Studies Using 3D Culture Models

Manipulation of the phenotype of normal and malignant cells cultured in 3D can provide valuable insight into cell communication pathways, and potential causes and treatments of cancer.

Pathway	**Description of Results**
Rap1 GTPase	Found to be crucial in organizing acinar structure and inducing lumen formation. Inhibition of Rap1 led to phenotypic reversion. [29]
β1-integrin	Inhibition of β1-integrin with blocking antibodies led to significan loss of cancer cell proliferation, increased apoptosis. Re-organized cytoskeletons. Non-malignant cells were resistant to any change. [30-32]
cAMP	cAMP analogues increased malignant cells' sensitivity to *Alu*I digestion, and to revert the structures to normal polarity. [33]
PI3K Kinase	Inhibition of PI3K reverted tissue polarity and decreased proliferation. Led to down-modulation of β1-integrin and EGFR, and up-regulation of PTEN. [34]
EGFR, MAPK	Reversion and reduced malignant behavior, decreased proliferation and increased polarity. [31]
PI3K Kinase	Normal cells with mutations to PI3K exhibit severe morphological deformities. [35]
ErbB2	ErbB2, but not ErbB1, reinititates proliferation and induces luminal repopulation in epithelial acini. [36]
Insulin-like growth factor	Type I insulin-like growth factor receptor overexpression led to large misshapen structures with filled lumena and disrupted polarization. [37]

It's been shown using 3D rBME cultures that regardless of growth status, in both malignant and nonmalignant mammary epithelial cells, the presence of the basement membrane provides protection from apoptosis. This suggests that integrin-induced polarity drives tumor-cell resistance to apoptotic agents via NFkB [38]. More specifically, the formation of polarized acini are dependent on the activity of α6 and β1 surface integrins, in combination with the presence of laminin-I [39]. Researchers have found a reciprocal cross-modulation between β1-integrin and EGFR which was not present in 2D cultures. This cross-modulation was attributed to being dependent on the presence of the basement membrane [40]. Experimentation with 3D cultures has led to the conclusion that apoptosis

must be restrained through resistance pathways for the lumen to become populated [41]. It was also found that luminal formation in rBME cultures required carcinoembryonic antigen—related cell adhesion molecule (CEACAM), to be present a high levels. This suggests that the morphogenic program integrates both cell-cell and cell-ECM signaling to produce the lumen [42]. The importance of MMP activity on branching morphogenesis was successfully demonstrated using 3D rBME cultures [43]. Similar *in vitro* models have been developed for other cell types, including skin, prostate, muscle, colon, bile duct, esophagus, adipocytes, fibroblasts, and embryonic stem cells [4]. Some of them are being used to study the same groups of pathways as well. For example, the disruption of the PI3K pathway has been found to have a similarly profound impact on the morphogenesis of epithelial acini in prostate cancer [44].

1.3 Mammalian Target of Rapamycin

To attempt to induce a normal phenotype for malignant cells, it was desired to select a compound with a great foundation of literary support to justify its selection, but also to design an original experiment. Rapamycin is the primary inhibitor for the mammalian target of rapamycin (mTOR) pathway. In a study using a non-cancerous breast epithelial cell line cultured in 3D with rBME, activation of the Akt kinase caused the cells to form morphologically disrupted structures with amplified proliferation. Inhibition with rapamycin completely reversed this malignant behavior [45]. Though rapamycin and other mTOR inhibitors are being investigated as cancer drugs, the effectiveness of mTOR

inhibition as a reversion strategy for breast cancer cell lines using rBME cultures appears to be unexplored. These are the reasons rapamycin was chosen for this study.

1.3.1 History of Use

Rapamycin was identified in the mid-1970s as a potent antifungal agent and was found to be a potent suppressor of the immune system. It was FDA approved in 1999 for use under the drug name Sirolimus as an immunosuppressive drug. Its immunosuppressive mechanism is derived from its inhibitory effect on the progression of T-cells from G1-phase into S phase [46]. Rapamycin is also being used to treat liver cirrhosis, and has proven effective in improvement of liver function in rat models, even in low doses [47]. Its structure is displayed in **Figure 3**. Its development as a cancer therapy has been far slower because of formulation and stability concerns in producing a parenteral formulation [48].

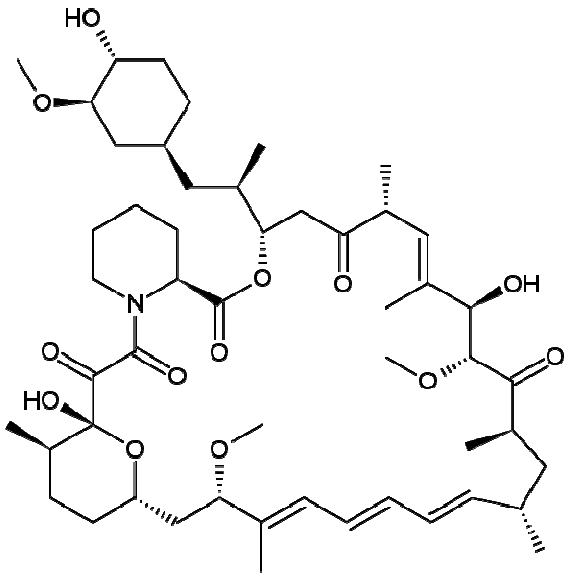

Figure 3: Structure of Rapamycin (Sirolimus)
Figure was released to Wikipedia.org as public domain.

In a study utilizing 3D rBME-embedded culture models, Akt activation elicited large, misshapen structures with enhanced proliferation and increased cell size. However, mTOR inhibition by rapamycin was shown to completely cancel these effects [49]. This study was the primary source for the selection of rapamycin as an exposure factor for reversion.

1.3.2 The Akt – mTOR Tango and Other Cancer Pathways

The serine/threonine kinase Akt (also known as PKB) is known to have at least three major impacts on cancer progression: proliferation, survival, and cell growth. For this reason, it is one of the most intensively studied pathways in breast cancer research. Down-regulation of Akt has been seen to inhibit anchorage-independent cell growth and induce apoptosis in various cancer cell lines [50]. Akt inactivates the downstream protein BAD, which normally promotes cell apoptosis in non-polarized cells [51]. PTEN, a tumor suppressor gene whose activity inhibits Akt phosphorylation, can be inhibited by mTOR. Therefore mTOR inhibition leads to PTEN *upregulation*, and hence Akt suppression [52].

The complex pathway web which includes mTOR, Akt, PI3K, and PTEN has been found to have various functions, including cell progression, angiogenesis, and resistance to apoptosis [53, 54]. Currently, rapamycin-chemotherapy pre-clinical combination studies are being conducted on mouse models to investigate rapamycin's effect on PI3K-induced cancers [55]. In prostate cells, doxorubicin resistance was reversed by rapamycin [56]. Rapamycin has been shown to reverse chemoresistance in lymphomas expressing Akt [57].

The effects of statins on Akt signaling was found only to be effective when used in combination with rapamycin [58].

The effects of mTOR on cancer pathways are not limited to Akt. Rapamycin exposure on mice was found to increase the levels of nitric oxide synthase in inflammatory responses. These effects appeared to be caused by mechanisms other than Akt [59], suggesting that mTOR has effects on other signal cascades. Rapamycin-induced inhibition of mTOR has been shown to inhibit MMP-7 production in mouse models [60], and MMP-9 has also been shown to be reduced by rapamycin exposure [61]. Increased MMP production is known to lead to breakdown of the ECM in many cases. In glioma cell lines, MMP-1, MMP-2, and MMP-9 was downregulated after treatment with rapamycin [62].

Inhibition of mTOR was found to have no effect on sensitivity to radiation therapy on glioblastoma cells when conducted in a monolayer, but was greatly increased when applied *in vivo* [63]. This further illustrates the importance of 3D cultures, while building the case for rapamycin as a cancer drug. Rapamycin exposure has also been shown to suppress tumor growth by anti-angiogenic suppression of vascular endothelial growth factor (VEGF) production [64]. In acute lymphoblast leukemia cells, rapamycin induced apoptosis and increased doxorubicin-induced apoptosis in many samples analyzed [65]. Cell proliferation tests demonstrated that rapamycin enhanced cell sensitivity to endocrine therapy in breast cancer cells [66].

Two distinct protein complexes are known to bind to mTOR: Raptor and Rictor. The mTOR-Raptor complex is exclusively downstream from Akt, while the mTOR-Rictor complex has a feedback mechanism by which it enhances Akt activity through PI3K and

PTEN. In effect, mTOR acts both downstream and upstream from Akt [67] in the signaling cascade. This is one very interesting aspect of the mTOR pathway, in that inhibiting it undoubtedly has multiple effects on cellular pathways.

1.4 Hypothesis & Aims

From the preceding literature review, the following hypothesis was formulated: Malignant cells, cultured in 3D rBME and exposed to rapamycin, can be forced to revert to a normal phenotype. Phenotypic reversion criteria include:

1. Decreased proliferation – smaller, growth-arrested colonies
2. Structural organization – spherical structures with increased multi-cellular organization and an ordered cytoskeleton
3. Polarization – increased interaction with the basement membrane and luminal formation in the center of the colonies

To conduct this experiment, two primary aims were developed:

1. Establishment of normal phenotype of normal cells cultured in 3D rBME as a positive control through optimization of culture conditions
2. Observing the effects of rapamycin on the phenotype of malignant cells cultured in 3D rBME.with comparisons to normal cells

CHAPTER 2

METHODOLOGY

There are two primary methods for conducting 3D culture with rBME gels. The first, embedded, involves fully embedding cells in a thick layer of gel, while the second, on-top, involves laying cells on-top a thin layer of gel while slowly adding additional gel in the media at low concentrations. Both methods allow 3D structure formation, but the on-top method has two advantages. First, it uses significantly less materials. Second, it lays all colonies into approximately the same horizontal plane. This makes image analysis significantly easier. For this study, only 3D on-top was used **(Figure 4)**. For more detailed descriptions of methods used, see Appendix A.

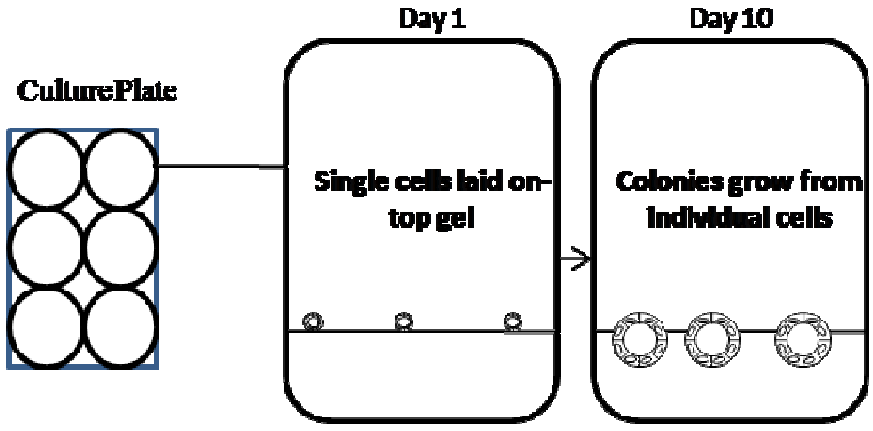

Figure 4: 3D on-top Method of Cell Culture
Individual cells are initially seeded on-top reconstituted rBME gels and supplemented with media containing 2-10% rBME v/v. Gel slightly thickens over time as more rBME is added every 2 days, and colonies grow into acini.

2.1 Cell Culture

Malignant breast epithelial cells (BT-483, MDA-MB-468) and normal breast epithelial cells (184-B5) were purchased from ATCC (VA). For monolayer culture, BT-483 was cultured using RPMI-1640 (Sigma-Aldrich, MO) with 20% fetal bovine serum (FBS) (Thermo Fisher Scientific, UT) and 0.01 mg/mL bovine insulin, MDA-MB-468 was cultured using Leibovitz's L-15 Media (Sigma-Aldrich) with 10% FBS in air with no added CO_2, and 184-B5 was cultured using MEGM (Lonza, Switzerland) with 1 ng/mL of cholera toxin and without gentamycin-amphotericin-B.

To achieve luminal morphology, cells were cultured using 3D on-top assays as previously described [68, 69]. The cultrex 3D culture matrix (Trevigen, MD) rBME product was chosen because it was specifically formulated for breast epithelial cell cultures and is modified to contain reduced growth factors and is phenol red free. Assay media was modified to contain 2-10% BME, with 2% FBS for malignant cells and with or without EGF (Epidermal Growth Factor) supplements for normal cells. All media was supplemented with 1% Penicillin/Streptomycin (Invitrogen, CA) and 0.1% Fungizone (Hyclone, UT). Cell cultures were seeded at $0.25x10^5$ (184-B5), $0.22x10^5$ (BT-483), and $0.18x10^5$ (MDA-MB-468) cells/cm^2. Assay media was changed every two days subsequent to seeding. Rapamycin (Sigma-Aldrich, MO) was reconstituted in DMSO and stored at -20°C at a stock concentration of 1 μM.

2.2 Morphological Observation

Morphology was observed using a TE2000-S Eclipse Microscope (Nikon, Japan) or a TS100 Eclipse Microscope (Nikon, Japan). All images were taken with a Digitial Sight DSQi1Mc Camera (Nikon, Japan). Fluorescence images were detected with an Intensilight C-HGFI lamp (Nikon, Japan). For the detection of non-viable (or apoptotic) cells, non-fixed cultures were incubated for 15-30 minutes with 1 µM ethidium bromide or 500 nM propidium iodide and observed for fluorescence. Cell colonies were extracted using PBS-EDTA solution, fixed using 4% paraformaldehyde, and blocked with 10% goat serum and 1% goat F(ab') IgG (Sigma-Aldrich, MO). Monoclonal anti-actin (1A4) and monoclonal anti-β-catenin (15B8) were obtained from Sigma-Aldrich (St. Louis, MO) for use as primary antibodies. Secondary antibody for FITC-conjugated goat anti-mouse was obtained from Santa Cruz Biotechnology (CA). Image analysis was conducted using NIS-Elements v3.0 (Nikon). Areas of cell colonies (in the x-y plane) in all images were analyzed for the calculation of mean areas under different conditions.

2.3 Caspase 3/7 Assay

Monolayers of BT-483 and 184-B5 cells were prepared in a 96-well plate to analyze the effects of RAP on caspase activity. Caspase activity was measured at 24 and 48 hours following exposure to RAP at 0, 5, and 20 nM. Exactly 100 µL of Casapase-Glo 3/7 Reagent (Promega, WI) was added to each sample, including 2 blank wells containing 100 µL of growth media and incubated for 2 hours. Luminescence was then measured using a Synergy 4 Plate Reader (Biotek, VT).

2.4 Cell Viability Assay

CellTiter-Blue Cell Viability Assay reagent was obtained from Promega (WI). MDA-MB-468 and 184-B5 cells were seeded in 96-well plates and, beginning on day two, were treated continuously with 0 nM and 20 nM RAP. On day three and day seven, cell viability assays were conducted and measured for fluorescence.

2.5 Real-Time RT-PCR Arrays

Human extracellular matrix and adhesion molecule-based real time reverse transcriptase polymerase chain reaction (RT-PCR) SuperArrays were obtained from SABiosciences (MD). MDA-MB-468 cells cultured in 3D on BME gels were treated with 0 nM and 20 nM RAP for six days. Colonies were extracted using PBS-EDTA, mRNA was extracted using RNeasy RNA isolation kit (QIAGEN, CA), and cDNA synthesis was conducted using the Reverse Transcriptase First Strand Kit (SABiosciences, MD). Real time PCR arrays were run using a Bio-Rad Opticon 2 thermocycler system (MJ Research, Canada) and analyzed using the Opticon 2 software provided. C_t values were acquired graphically.

2.6 Statistical Analysis

With the SYSTAT 12 software, statistical analyses on all quantitative data were carried out using one-way and two-way ANOVA (analyses of variance) to verify statistical significance ($p < 0.05$).

CHAPTER 3

RESULTS

3.1 Optimization of Culture Conditions

Using the 3D on-top method, 184-B5 (normal) cells were initially cultured in a MEGM-based assay medium containing epidermal growth factor (EGF) additive, a supplement provided with the Media kit. Cultured cells formed large, morphologically disrupted structures with no apparent limitations to growth. Culturing the cells in EGF-reduced media resulted in the formation of significantly smaller structures with uniformity in shape. This effect is demonstrated in **Figure 5**. EGF-reduced cultures appeared to reach a maximum size by day 6 of culture. Exposure to 20 nM rapamycin had no visible effect on EGF-induced morphological distortion.

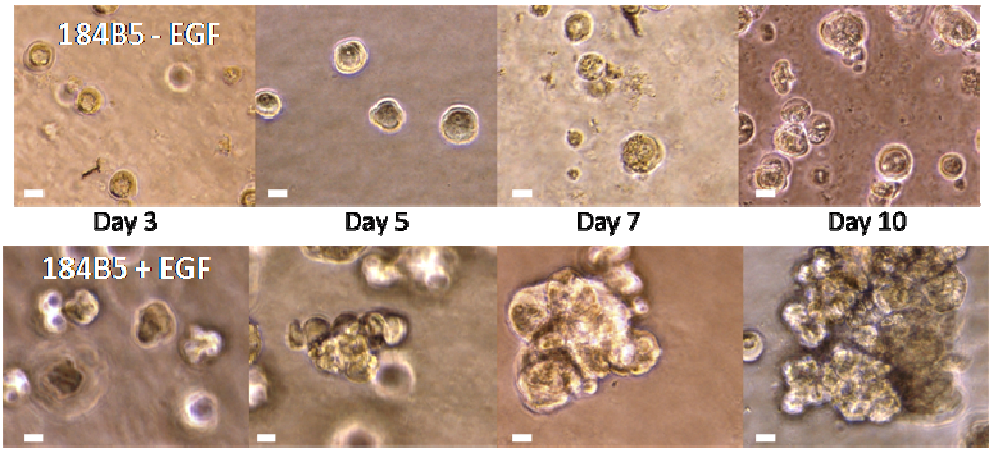

Figure 5. Effects of EGF on 3D Morphology of Normal Cells
184B5 breast epithelial cells cultured on-top BME gels with and without EGF. **Top**, EGF-reduced assay media induced a normal phenotype, including smaller, round morphology with maximum size by day 5 of culture. **Bottom**, EGF-enhanced assay media leads to increased proliferation and disrupted morphology. (Scale bars = 25 µm)

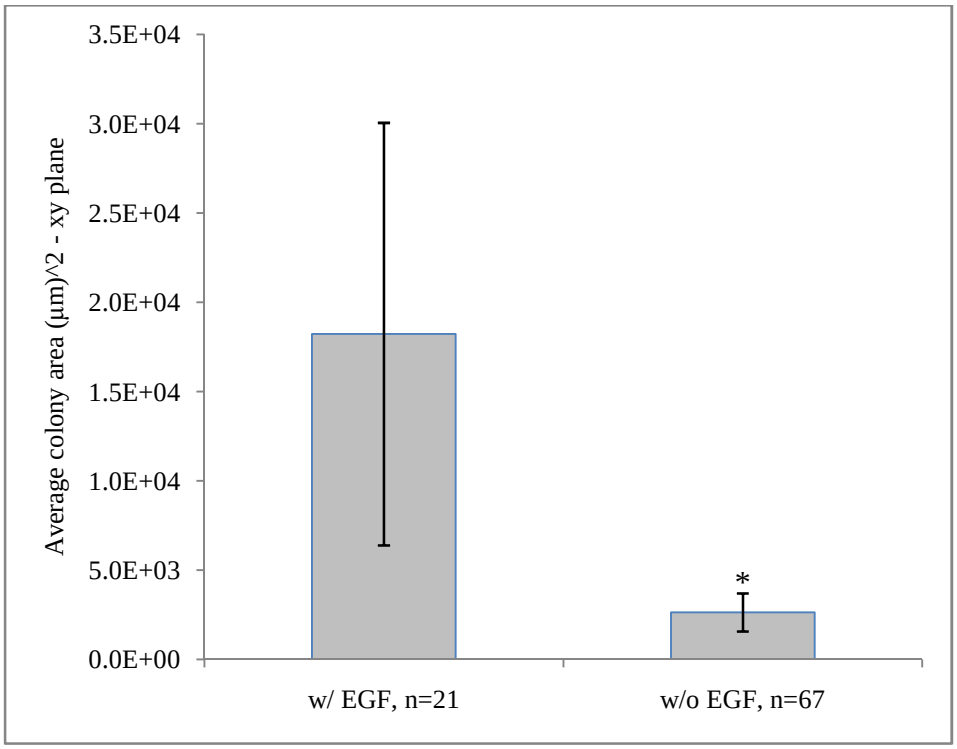

Figure 6. Effects of Reducing EGF on Average Colony Size for Normal Cells
Average cell colony areas were measured from 184B5 breast epithelial cells cultured on-top BME gels with and without EGF on day 7 of culture. EGF-reduced colonies showed a significantly lower average area than the EGF-enhanced colonies. (* Significantly lower than control, Error bars $\pm$ st. dev, $p < 0.05$)

Image analysis of average area of normal cells with and without EGF showed a significantly lower area for EGF-reduced colonies at day 7 (**Figure 6)**. This proves quantitatively that EGF causes over-proliferation and prevents proper formation of the normal phenotype.

Malignant cells cultured using the 3D on-top method grew into large, morphologically disrupted structures. Unlike EGF reduction, FBS reduction did not lead to a change in morphology. Subsequently, 2% FBS was used in all experiments.

3.2 Effects of Rapamycin Exposure

3.2.1 Caspase 3/7 Activity

Figures 7 and 8 show the effects of rapamycin exposure on caspase activity in normal (184-B5) and malignant (BT-483) breast epithelial cells. For normal cells, the only condition which showed significant deviation fom the control was 20 nM rapamycin for 48 hours of exposure. For malignant cells, 20 nM of exposure showed a significantly higher effect on caspase activity than 5 nM, but only at 48 hours of exposure. Caspase 3 and caspase 7 are established markers for programmed cell death. Programmed cell death is required for the formation of the luminal space in 3D cultures, so this data provides evidence that rapamycin can have an effect on polarity. For raw data, see Appendix B.

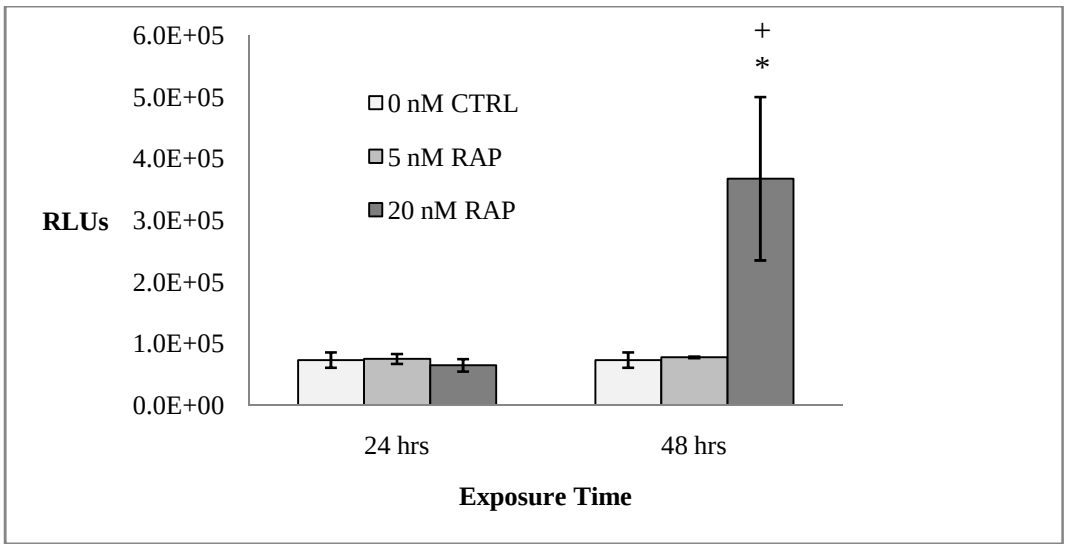

Figure 7: Caspase 3/7 Response in Normal Cells From Rapamycin Exposure
Effect on caspase activity of normal (184-B5) breast epithelial cell monolayers at 24 and 48 hours of exposure to 0, 5, and 20 nM rapamycin. (n=2, * significantly higher than control, + significantly higher than 5 nM, error bars $\pm$ st. dev., $p < 0.05$)

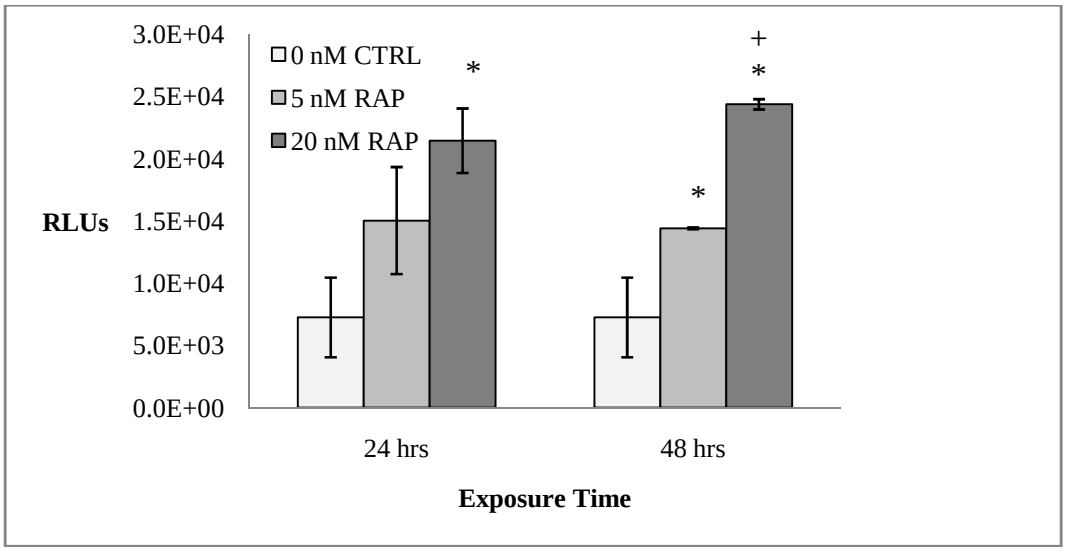

Figure 8: Caspase 3/7 Response in Malignant Cells From Rapamycin Exposure Effect on caspase activity of malignant (BT-483) breast epithelial cell monolayers at 24 and 48 hours of exposure to 0, 5, and 20 nM rapamycin. (n=2, * significantly higher than control, + significantly higher than 5 nM, error bars $\pm$ st. dev., $p < 0.05$)

3.2.2 Cell Viability Assay

Figure 9 shows the effects of 20 nM rapamycin on the total level of cell viability in monolayer cultures of both normal (184-B5) and malignant (MDA-MB-468) cells after 2 and 6 days of continuous exposure (and one day untreated). Both cell lines (MDA-MB-468 & 184-B5) showed a significant reduction in cell proliferation with a significantly higher reduction seen on day 7 than on day 3. This shows that Rapamycin has either a cytotoxic effect, or that it leads to downstream regulation of the cell cycle. The caspase data previously shown provides evidence that the latter is true. All conditions were conducted in triplicates. Error bars show the standard deviation among the three samples, and in all cases there is no overlap between the error bars of the control and treatment samples. This data shows a significant change in viable cells in each of the treated samples conditions

($p<0.05$). This is quantitative supporting evidence that rapamycin limits cell proliferation, at an increasing margin over time. For raw data, see Appendix B.

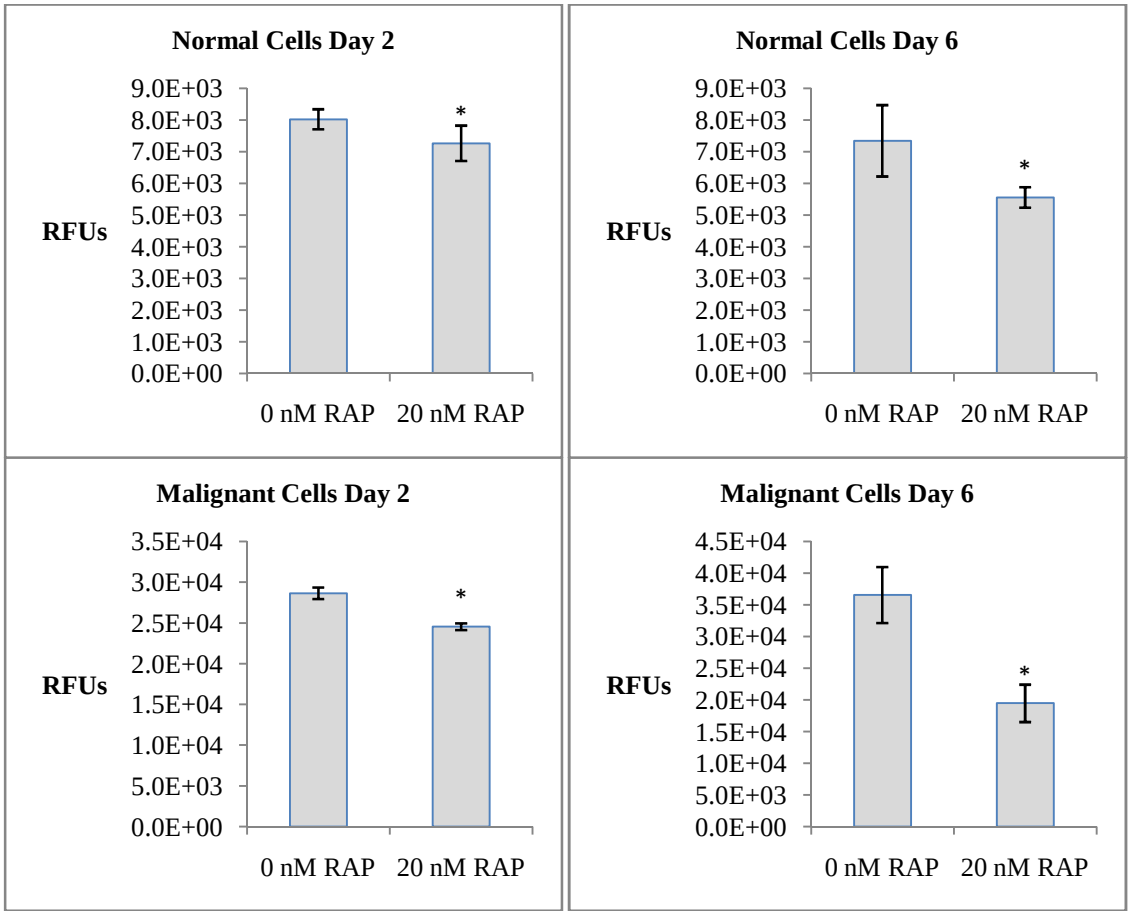

Figure 9: Proliferation of Normal and Malignant Cells at 2 & 6 Days of Rapamycin Exposure

Monolayer cultures of normal (184-B5) and malignant (MDA-MB-468) cells were exposed for 2 & 6 days to 20 nM rapamycin, and analyzed for total cell viability. Levels of cell viability were significantly lower under all conditions for rapamycin-treated cultures, by an increasing margin over time. (n=3, * significantly lower than control, $p < 0.05$)

3.2.3 Morphological Observation

Exposure with 20 nM rapamycin led to an average of considerably smaller sized cell colonies, typically reaching their maximum size by day 6 (**Figure 10).** Cell colonies were comparable in size and shape to normal cells. Rapamycin exposure led to significant reduction of average cell colony area (**Figure 11)** in both malignant cell lines (BT-483 & MDA-MB-468).

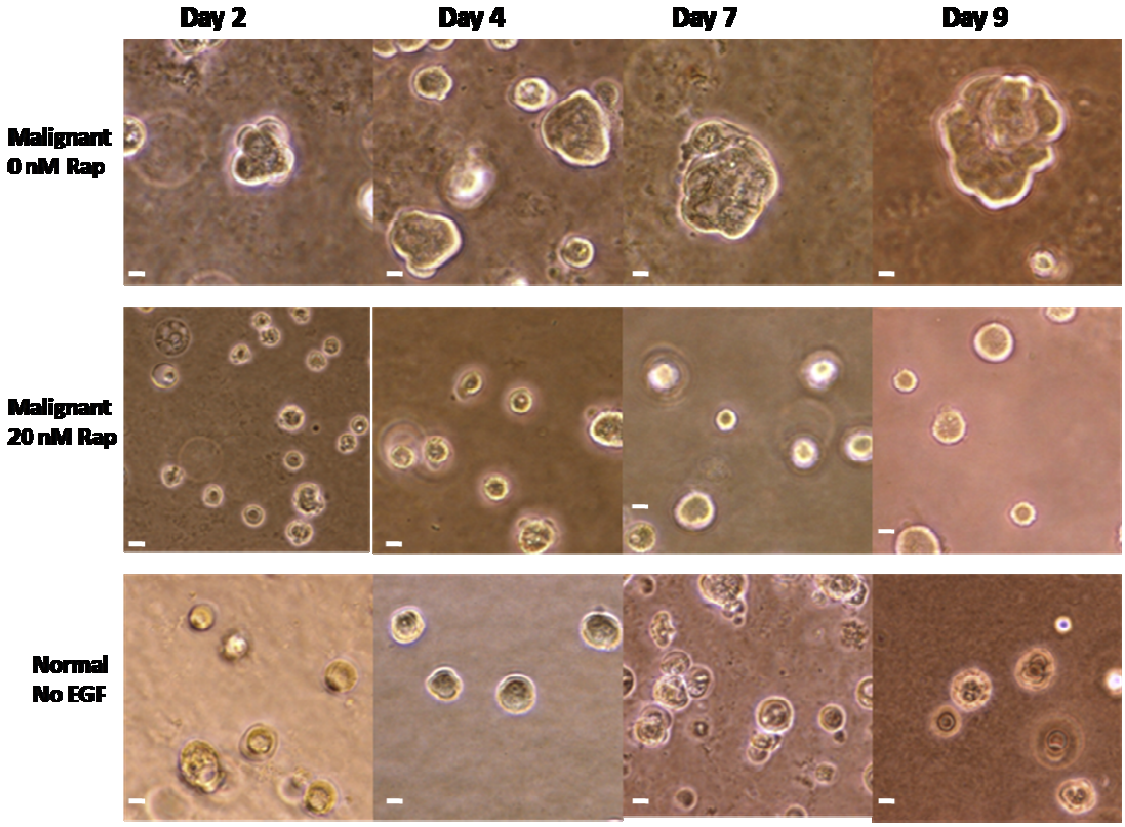

Figure 10. Effect of Rapamycin Exposure on Malignant Cell Morphology in 3D Culture

Rapamycin was exposed to malignant (BT-483) cells beginning after one day of culture at 0 and 20 nM concentrations, and compared to normal (184-B5) cells. Normal cells, **bottom**, compared in colony shape and size to rapamycin-treated cultures, **middle**. Malignant cells, **top**, exhbited severe morphological disruption when cultured without treatment. (Scale bars = 25 μm)

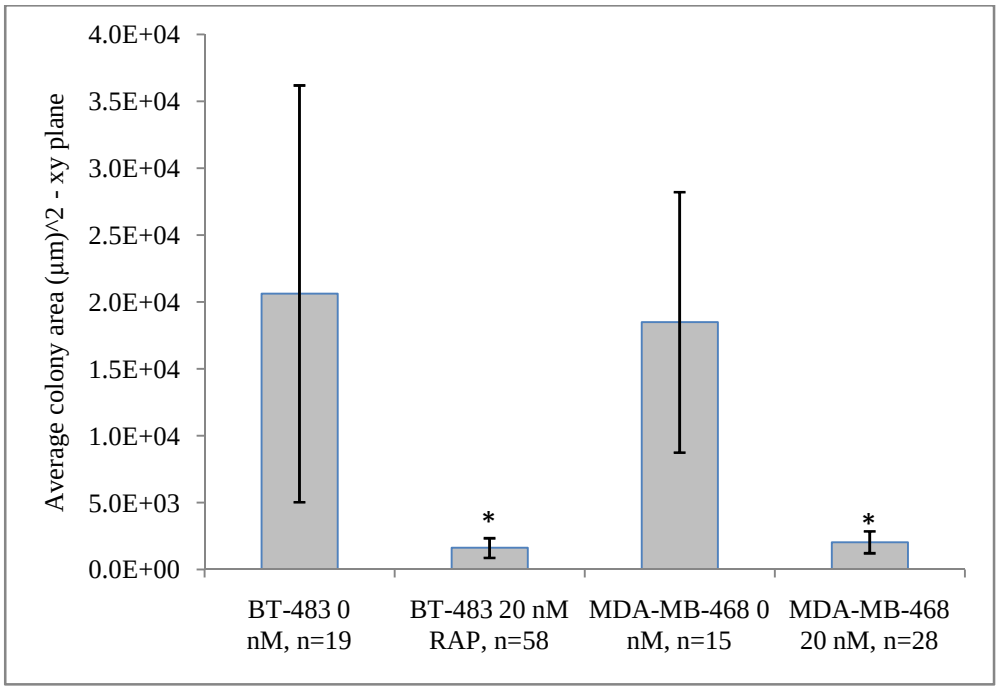

Figure 11. Effects of Rapamycin Exposure on Average Cell Colony Size of Malignant Cells on Day 7 of 3D Culture

Effects of rapamycin exposure on average cell colony size: Average cell colony areas were measured from malignant (BT-483 & MDA-MB-468) cells continuously treated with 0 and 20 nM rapamycin Average cell colony areas (xy plane) were measured from BT-483 and MDA-MB-468 malignant cells treated with 0 and 20 nM RAP on day 7 of 3D rBME culture. No significant difference was found between the two cell lines, but rapamycin treatment significantly reduced cell colony size. (Error bars $\pm$ st. dev, * significantly lower than control, $p < 0.05$).

Labelling of apoptotic cells was done using ethidium bromide and propidium iodide to stain un-fixed 3D cultures of normal and malignant cells (**Figure 12**) at day 8 of culture. An inner subset of cells undergoing luminal cell death (apoptosis) was observed in normal cell colonies, as well as malignant cell colonies treated continuously with rapamycin. This indicates the presence of lumen formation, and provides evidence that rapamycin treatment induced the cells to exhibit polarity.

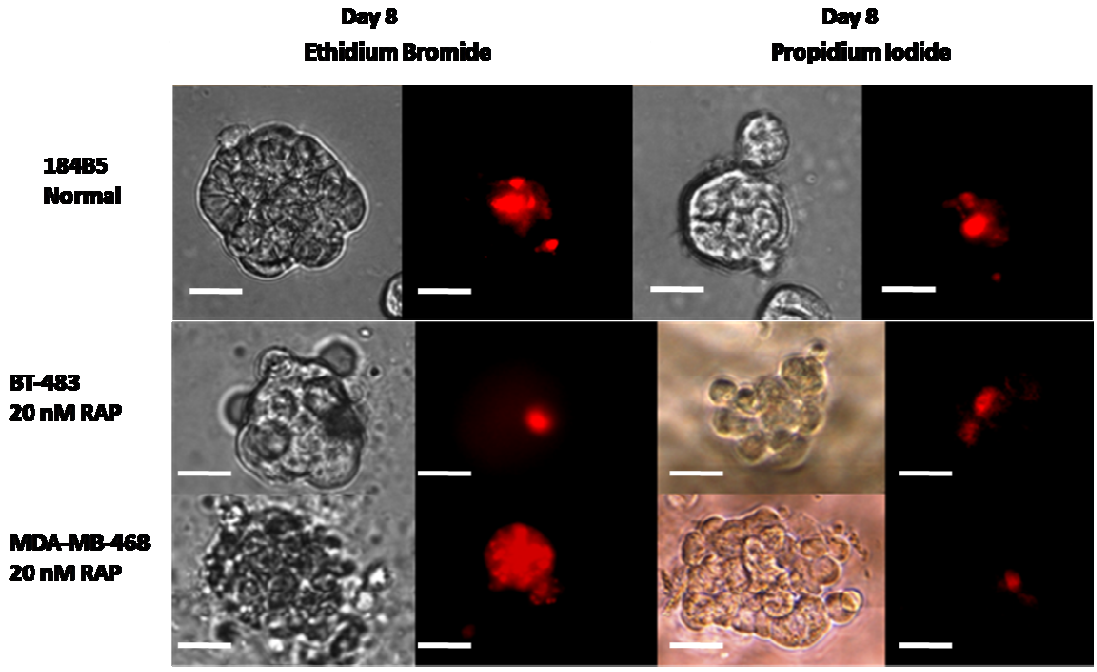

Figure 12. Selective Staining of Non-Viable Cells Indicates the Presence of Luminal Apoptosis

Top: Staining of day 8 3D cultures of normal (184-B5) cells with ethidium bromide or propidium idodie resulted in detection of cell death in the center of cell colonies.
Bottom & Middle: Similar occurences of centrally-localized apoptosis were detected in both cancer cell lines (BT-483 & MDA-MB-468) when treated continuously with 20 nM rapamycin. (Scale bars = 25 µm)

Structural organization was observed using anti-actin and anti-β-catenin immunofluorescent stains. The results are pictured in **Figure 13**. Cells were stained with FITC secondary antibodies (green) and counterstained with DAPI (blue). Reverted malignant cells and normal cells exhibited primarily spherical multi-cellular colonies, while untreated malignant cells showed no organization. Rapamycin-treated malignant colonies exhibited cells arranged around the center, showing similarities to the structure of normal cells cultured in rBME.

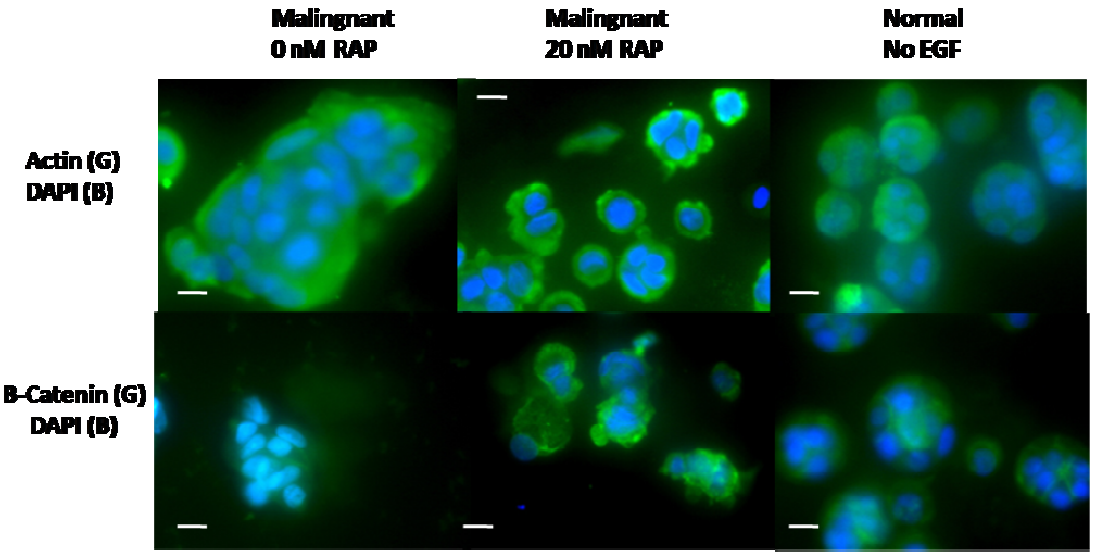

Figure 13. Immunofluorescent Staining of Normal Cells and Rapamycin Treated Malignant Cells at Day 7 of 3D Culture

Malignant (BT-483) cell colonies from day 7 of culture, after continuous treatment of 20 nM rapamycin from day 2, exhibit multi-cellular organization similar to day 7 cultures of normal (184-B5) cells.
Top: Anti-actin (green) counterstained with DAPI (blue).
Bottom: Anti-β-batenin (green) counterstained with DAPI (blue). (Scale bars = 25 µm)

3.2.4 RT-PCR Arrays

Two PCR array plates containing genes related to human extracellular and adhesion molecules were run together with cDNA derived from mRNA extracted from HTB-132 cells grown in rBME. One sample, as a control, was untreated. The other sample was exposed to 20 nM rapamycin for four days after two days untreated. The PCR arrays included six wells for positive controls and one well for a genomic DNA contamination check. The genomic DNA contamination wells were both >35, which indicates that there was no genomic DNA contamination. The standard deviation for all controls were well below 1, as was the difference between the average controls for the two plates. The

difference between the reverse transcription control (RTC) and the positive PCR control (PPC) was $\leq$ 5, which designates the presence of successful PCR reactions. From these calculations, it was concluded that the data is acceptable for analysis. See appendix for raw data and quality control analysis.

Ct values were cutoff at $\geq$ 35 as undetected. Fold change of each gene was calculated using the DDCT ($\Delta\Delta$Ct) and classified according to gene category (**Table 2**). Data was cutoff as significant at a fold change of $\leq$ 0.2 or $\geq$ 5.0. See appendix for additional tables containing genes inside the cutoff range, and genes for which no fold change could be calculated due to a Ct value of $\geq$ 35.

Twenty-five genes related to ECM & adhesion molecules showed a significant (at least 5-fold) increase in expression, while no genes showed a significant (less than 0.2) decrease in expression. Gene groups including basement membrane constituents and cell-matrix adhesion molecules support the presence of increased basolateral polarity in 3D cultured malignant cells treated with 20 nM rapamycin. Gene groups including cell-cell adhesion molecules, trans-membrane molecules, and other adhesion molecules such as catenin support the presence of increased structural organization in 3D cultured malignant cells treated with 20 nM rapamycin.

Table 2. Rapamycin's Effects on Gene Expression of Human Extracellular Matrix and Adhesion Molecules

Fold change was calculated using the DDCT method, with GADPH as the normalizing gene. See Appendix B for complete data.

Gene Category	Symbol	Description	Fold Change
Basement Membrane Constituents	LAMA2	Laminin, alpha 2	13.77
	LAMA3	Laminin, alpha 3	19.05
	LAMB3	Laminin, beta 3	12.57
	SPARC	Secreted protein, acidic, cysteine-rich	13.64
Cell-Cell Adhesion	CDH1	Cadherin 1, type 1, E-cadherin (epithelial)	6.40
	CTNND1	Catenin (cadherin-associated protein), delta 1	7.13
Cell-Matrix Adhesion	CD44	CD44 molecule (Indian blood group)	6.95
	ITGA2	Integrin, alpha 2	9.84
	ITGA6	Integrin, alpha 6	5.26
	ITGAV	Integrin, alpha V	8.99
	ITGB1	Integrin, beta 1	14.30
	ITGB2	Integrin, beta 2	9.27
	ITGB5	Integrin, beta 5	5.48
	SGCE	Sarcoglycan, epsilon	5.25
Collagens & ECM Structural Constituents	COL1A1	Collagen, type I, alpha 1	5.79
	COL4A2	Collagen, type IV, alpha 2	9.77
	FN1	Fibronectin 1	16.51
ECM Protease Inhibitors	THBS1	Thrombospondin 1	16.02
Other Adhesion Molecules	COL12A1	Collagen, type XII, alpha 1	17.50
	CTNNA1	Catenin (cadherin-associated protein), alpha 1	7.82
	CTNNB1	Catenin (cadherin-associated protein), beta 1	11.40
	LAMC1	Laminin, gamma 1 (formerly LAMB2)	6.36
Other ECM Molecules	TGFBI	Transforming growth factor, beta-induced, 68kDa	10.04
	VCAN	Versican	17.70
Trans-membrane Molecules	ITGA4	Integrin, alpha 4	5.87

CHAPTER 4

DISCUSSION

As shown in **Figure 14,** normal phenotype was achieved in 3D rBME cultures through elimination of EGF in normal cells, and through exposure to rapamycin in malignant cells. To reach this conclusion, we applied the results to three criteria as established in the introduction – structural organization, limited proliferation, and polarity.

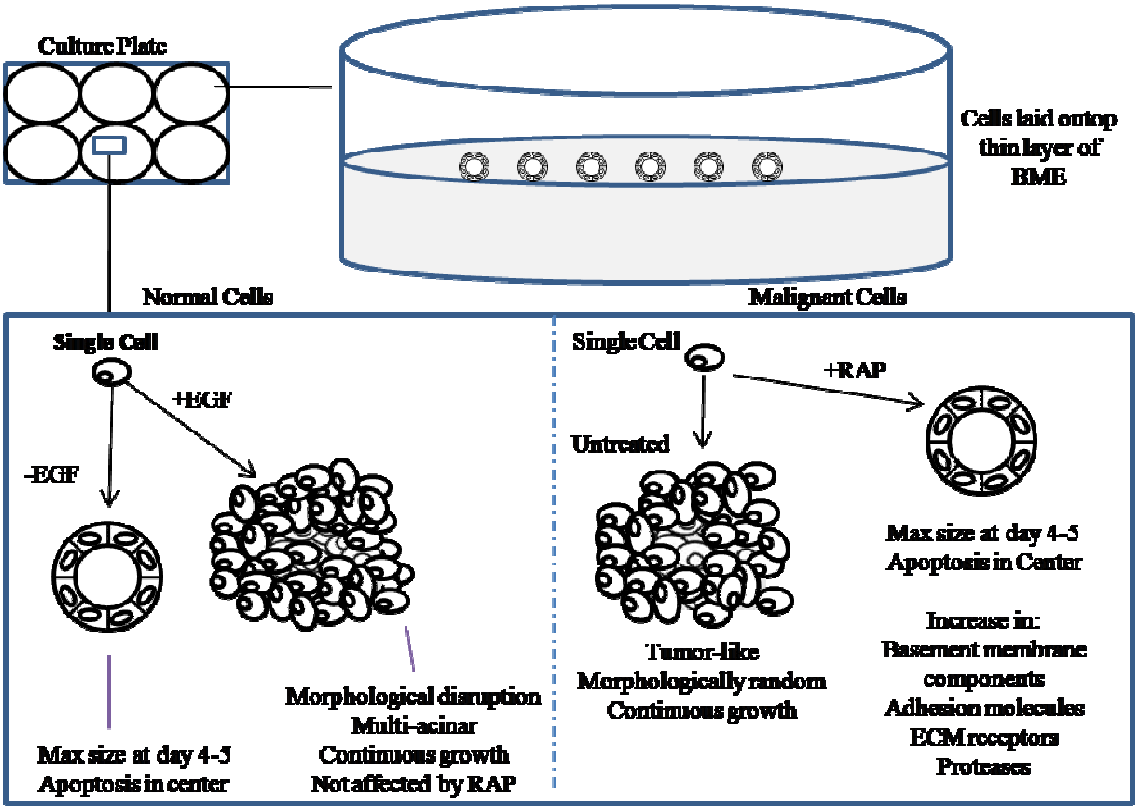

Figure 14. Summary of Experimental Results
In normal cells, normal phenotype was achieved by removing EGF additive from the assay media, leading to limited proliferation, maximum cell colony size, and luminal apoptosis. Rapamycin limited proliferation of malignant cells and induced luminal apoptosis. RT-PCR analysis showed an increase in gene expression of many molecules important to polarity and structural organization, including basement membrane components, cell-matrix adhesion molecules, and cell-cell adhesion molecules.

Increased multi-cellular organization was observed in the anti-actin and anti-β-catenin immunostaining images. The change in shape of the colonies from amorphous to round is the strongest evidence towards satisfying this criterion. An increase in structural organization was also supported by an increase in expression of genes related to cell-cell adhesion molecules and ECM structural constituents.

Limitations on proliferation were observed through morphological observation as well, and were confirmed by the significant change in the average areas measured in 3D cell cultures treated with rapamycin. The cell viability assay data also provided evidence of a decrease in proliferation due to rapamycin.

Evidence of increased polarity due to rapamycin exposure was provided by the images of apoptotic cells located in the center of several cell colonies, indicating the formation of a lumen. The observed increase in caspase activity provides evidence that rapamycin affects the cell cycle and forces programmed cell death. Finally, an observed increase in expression of genes related to basement membrane constituents and cell-matrix adhesion molecules provides additional evidence that polarization is taking place.

Both qualitative and quantitative data was gathered to support all three criteria. Note that, in some previous studies, reversion has been concluded though only one or two of these criteria were satisfied [1, 9, 30, 31]. Therefore, a conclusion can be made that Rapamycin exposure, in combination with rBME surroundings and serum-reduced media, can revert malignant cells to show a normal phenotype in 3D cultures.

4.1 Drawbacks to the Study

While the caspase and cell viability assays provided valuable insight into the effects of rapamycin exposure, this study would have benefited from similar data derived from 3D cultures. Both assays were attempted on 3D cultures, but failed to yield results with significant difference from the controls. The ECM gel may have been autofluorescing / autoluminescing. It is also possible that the assay reagents were either being absorbed by (or failing to penetrate) the ECM, or were reacting with the ECM. Assays which could be conducted on cells extracted from the ECM would likely have been much more effective.

The study would also have benefited from immunostaining images with observed localization of function. Actin and β-catenin were not specifically localized, but present all throughout the colonies. Antibodies for molecules related to polarity, such as α6-integrin, would likely have been observed around the periphery of the colonies. Such localization would likely have only been possible with confocal microscopy.

Furthermore, more replicates of the RT-PCR arrays would have statistically strengthened the gene expression data. However, great confidence is placed in commercially distributed PCR arrays, and researchers often publish data from a single set of PCR arrays if they come from a trusted manufacturer.

Another drawback to this study is derived from the variability between different cell lines, which include morphological properties and nutrition requirements. A previous study classified malignant cell lines into four main classifications by morphology, which differ significantly in genotype [3]. The two cell lines used in this study had “mass” and

"grape-like" morphologies, but we cannot be certain whether rapamycin exposure would be effective on the other morphology types, "round" and "stellate".

When initially culturing normal (184-B5) cells, growth-arrested spherical acini were not observed. Decreasing the amount of growth factors in the media by removing the EGF supplement prevented this. Likely, the presence of such a high level of growth factors led to an override of pathways which limit proliferation and lead to increased cellular cooperation and structural organization. In addition to growth factors, these cultures are very sensitive to humidity, and dry out much easier than 2D cultures do.

While this culture system has increased complexity when compared to plastic-bound monolayers, it is still profoundly simple when compared to real breast tissue. Only one cell type, epithelial, is represented in this model, while real breast tissue contains many other cell types, including myoepithelial cells, fibroblasts, and adipose (fat) tissue. Co-cultures of adipocyte/epithelial cells have been attempted [70]. There are many challenges in attempting such heterotypic cell cultures. Accounting for the different metabolic and nutritional requirements would be a difficult task indeed, and would require much experimentation to optimize. Another difficulty is that in actual tissue, cell types are separated from each other, such as epithelial cells from stromal cells by a basement membrane, but in co-cultures the cell types would be co-mingled. Finally, co-cultures containing normal and malignant cells together would need methods to control the ratios of cells, as they may grow at different rates [4].

4.2 Future Direction

Rapamycin has shown evidence of phenotypic reversion, but it is not the only mTOR inhibitor. Rapamycin is actually a poor parenteral drug, due to its poor water solubility and limited stability. Three analogues have been developed with improved pharmaceutical properties: CCI-799 (tensirolimus), RAD-001 (everolimus) and AP-23573 (deforolimus, ARIAD). All three are more effective orally and are currently under drug trials [71, 72]. These derivatives should also be investigated for their effectiveness as reversion factors [52].

In addition, it would to be interesting to observe the effects of combining rapamycin with other signal molecules to see their combined or synergistic effects on reversion of breast cancer cells [73]. Such combination strategies for reversion have been done many times before [9]. Rapamycin's synergistic effects with paclitaxel, carboplatin, and vinorelbine have been observed in a few breast cancer lines *in vitro* [53]. Mullerian inhibiting substance (MIS) has also been tested with rapamycin as a dual strategy for fighting ovarian cancer. Additive effects on MIS's protein targets were observed [74] and assumed to be synergistic. The additive effects of combined exposure with doxorubicin and gemcitabine synergistically enhanced chemotherapy-induced cytotoxicity in breast cancer cells [75]. These studies suggest that doxorubicin, paclitaxel, carboplatin, vinorelbine, gemcitabine, and MIS would be valuable candidates for such a combination strategy.

Three-dimensional cultures could be used to observe the mechanical properties of normal and malignant breast cells. Such studies are currently being conducted [12, 76], and can have far-reaching new insights on the development of tumors, including potential new methods of treatment. If oncogenic behavior can be induced by applying external mechanical forces, it would give valuable insight into the importance of tissue microenvironment on tumor progression [8].

Surgeons attempting breast-conservation therapy (BCT) for breast cancer patients would benefit greatly from an effective device for the detection of cancerous tissue in margins of extracted tumors, and the frequency of remission cases would be drastically cut. Ultrasound detection provides a promising option: it is relatively cheap and noninvasive [77]. Currently, mathematical models exist which attempt to explain patterns of cell configurations utilizing the single cell as the basic unit [78]. Testing indicates that as few as 300 malignant cells in a tissue sample can be detected [79]. The model takes advantage of the fact that malignant cells have significantly larger nuclei than normal cells. A distinct correlation between the size of the nuclei and integrated backscatter coefficient values has been found through experimentation. In addition, apoptotic cells affect ultrasound readings [80]. This is likely due to the destructive interference resulting from greater randomization of cell nuclei [81].

Three-dimensional co-cultures of normal and malignant cells should be developed for testing these ultrasound models. However, there are challenges involved. First, a uniformly distributed numerical model may not translate properly into a tissue sample or a cell-based model. In actual tissue, and in these cultures, there is little uniformity, due to the

complex architecture these cells arrange. Numerical models being proposed include both ordered lattices and randomized microstructures [82] to address this issue, but exactly how these numerical models will fare when applied to gel models will depend on several conditions. It should first be confirmed that the normal cells being used in the co-culture have significantly smaller nuclei than the malignant cells. If accurate measurement shows that the immortalized cell line used in this study also possesses enlarged nuclei, it may be better to acquire primary cells for use in co-culture. The second issue is whether the cell ratio can be easily controlled in a co-culture. It is already established from this study that cultures of one cell type can be controlled through modification of growth factors and other additives in the media, and through growth inhibitors such as rapamycin. However, the control of one cell type may lead to negative side effects on the other cell type, especially when the cell lines use different media. A promising side effect which was noticed during this study was that normal cells appeared unaffected by rapamycin when in 3D culture. This suggests that rapamycin may be a useful control factor for co-cultures.

4.3 Conclusion

In this study, the effects of rapamycin exposure on the phenotypic reversion of malignant breast epithelial cell lines were investigated using a 3D rBME culture system. Microscopic observation of malignant 3D cell cultures treated with rapamycin showed greater similarities in morphology to normal cell cultures than in untreated malignant cultures. Comparison of the average horizontal areas of untreated and rapamycin-treated malignant cell colonies confirmed that rapamycin-treated malignant cell colonies are

significantly smaller in size. Increased structural organization was observed by immunofluorescent staining of anti-actin and anti-β-Catenin. On day 8 of 3D rBME cultures, rapamycin-treated malignant cells stained with ethidium bromide showed similar occurrences of luminal cell death to that observed in normal cultures, indicating re-polarization of the epithelial cell layer. Supporting data from monolayer cultures indicated that levels of caspase activity was increased in the presence of rapamycin, and that proliferation over time was decreased. Gene expression analysis of rapamycin-treated malignant cells from 3D culture indicated an increase in the expression of several ECM or adhesion molecules important to polarity and structural organization. This collection of data supports our hypothesis that RAP exposure can revert malignant breast epithelial cells to a normal phenotype.

Our study has provided data supporting the value of mTOR inhibition as a potential anti-tumor strategy. To provide further insight into mTOR inhibition, two further directions of research should be taken: additional studies on the effects of other mTOR inhibitors on phenotypic reversion, and combination studies to investigate the synergistic or combined effects of mTOR inhibition with other cancer targets.

REFERENCES

1. Schmeichel, K.L. and Bissell, M.J. Modeling tissue-specific signaling and organ function in three dimensions. J Cell Sci **116**, 2377, 2003.

2. Xu, F. and Burg, K.J. Three-dimensional polymeric systems for cancer cell studies. Cytotechnology **54**, 135, 2007.

3. Kenny, P.A., Lee, G.Y., Myers, C.A., Neve, R.M., Semeiks, J.R., Spellman, P.T., Lorenz, K., Lee, E.H., Barcellos-Hoff, M.H., Petersen, O.W., Gray, J.W., and Bissell, M.J. The morphologies of breast cancer cell lines in three-dimensional assays correlate with their profiles of gene expression. Mol Oncol **1**, 84, 2007.

4. Weigelt, B. and Bissell, M.J. Unraveling the microenvironmental influences on the normal mammary gland and breast cancer. Semin Cancer Biol **18**, 311, 2008.

5. Sonnenschein, C. and Soto, A.M. Carcinogenesis and metastasis now in the third dimension--what's in it for pathologists? Am J Pathol **168**, 363, 2006.

6. Ghajar, C.M. and Bissell, M.J. Extracellular matrix control of mammary gland morphogenesis and tumorigenesis: insights from imaging. Histochem Cell Biol **130**, 1105, 2008.

7. Bissell, M.J., Weaver, V.M., Lelievre, S.A., Wang, F., Petersen, O.W., and Schmeichel, K.L. Tissue structure, nuclear organization, and gene expression in normal and malignant breast. Cancer Res **59**, 1757, 1999.

8. Bissell, M.J. Modelling molecular mechanisms of breast cancer and invasion: lessons from the normal gland. Biochem Soc Trans **35**, 18, 2007.

9. Bissell, M.J., Rizki, A., and Mian, I.S. Tissue architecture: the ultimate regulator of breast epithelial function. Curr Opin Cell Biol **15**, 753, 2003.

10. Roskelley, C.D., Desprez, P.Y., and Bissell, M.J. Extracellular matrix-dependent tissue-specific gene expression in mammary epithelial cells requires both physical and biochemical signal transduction. Proc Natl Acad Sci U S A **91**, 12378, 1994.

11. Paszek, M.J., Zahir, N., Johnson, K.R., Lakins, J.N., Rozenberg, G.I., Gefen, A., Reinhart-King, C.A., Margulies, S.S., Dembo, M., Boettiger, D., Hammer, D.A., and Weaver, V.M. Tensional homeostasis and the malignant phenotype. Cancer Cell **8**, 241, 2005.

12. Butcher, D.T., Alliston, T., and Weaver, V.M. A tense situation: forcing tumour progression. Nat Rev Cancer **9**, 108, 2009.

13. Kumar, S. and Weaver, V.M. Mechanics, malignancy, and metastasis: the force journey of a tumor cell. Cancer Metastasis Rev **28**, 113, 2009.

14. Le Beyec, J., Xu, R., Lee, S.Y., Nelson, C.M., Rizki, A., Alcaraz, J., and Bissell, M.J. Cell shape regulates global histone acetylation in human mammary epithelial cells. Exp Cell Res **313**, 3066, 2007.

15. Talhouk, R.S., Bissell, M.J., and Werb, Z. Coordinated expression of extracellular matrix-degrading proteinases and their inhibitors regulates mammary epithelial function during involution. J Cell Biol **118**, 1271, 1992.

16. Nelson, C.M., Khauv, D., Bissell, M.J., and Radisky, D.C. Change in cell shape is required for matrix metalloproteinase-induced epithelial-mesenchymal transition of mammary epithelial cells. J Cell Biochem **105**, 25, 2008.

17. Nelson, C.M. and Bissell, M.J. Of extracellular matrix, scaffolds, and signaling: tissue architecture regulates development, homeostasis, and cancer. Annu Rev Cell Dev Biol **22**, 287, 2006.

18. O'Brien, L.E., Zegers, M.M., and Mostov, K.E. Opinion: Building epithelial architecture: insights from three-dimensional culture models. Nat Rev Mol Cell Biol **3**, 531, 2002.

19. Silberstein, G.B. Tumour-stromal interactions. Role of the stroma in mammary development. Breast Cancer Res **3**, 218, 2001.

20. Gudjonsson, T., Ronnov-Jessen, L., Villadsen, R., Rank, F., Bissell, M.J., and Petersen, O.W. Normal and tumor-derived myoepithelial cells differ in their ability to interact with luminal breast epithelial cells for polarity and basement membrane deposition. J Cell Sci **115**, 39, 2002.

21. Reginato, M.J. and Muthuswamy, S.K. Illuminating the center: mechanisms regulating lumen formation and maintenance in mammary morphogenesis. J Mammary Gland Biol Neoplasia **11**, 205, 2006.

22. Ronnov-Jessen, L., Petersen, O.W., and Bissell, M.J. Cellular changes involved in conversion of normal to malignant breast: importance of the stromal reaction. Physiol Rev **76**, 69, 1996.

23. Petersen, O.W., Ronnov-Jessen, L., Howlett, A.R., and Bissell, M.J. Interaction with basement membrane serves to rapidly distinguish growth and differentiation pattern of normal and malignant human breast epithelial cells. Proc Natl Acad Sci U S A **89**, 9064, 1992.

24. Barcellos-Hoff, M.H., Aggeler, J., Ram, T.G., and Bissell, M.J. Functional differentiation and alveolar morphogenesis of primary mammary cultures on reconstituted basement membrane. Development **105**, 223, 1989.

25. Patrick, C.W., Jr. and Wu, X. Integrin-mediated preadipocyte adhesion and migration on laminin-1. Ann Biomed Eng **31**, 505, 2003.

26. Li, S., Edgar, D., Fassler, R., Wadsworth, W., and Yurchenco, P.D. The role of laminin in embryonic cell polarization and tissue organization. Dev Cell **4**, 613, 2003.

27. Kleinman, H.K., McGarvey, M.L., Liotta, L.A., Robey, P.G., Tryggvason, K., and Martin, G.R. Isolation and characterization of type IV procollagen, laminin, and heparan sulfate proteoglycan from the EHS sarcoma. Biochemistry **21**, 6188, 1982.

28. Timpl, R., Rohde, H., Robey, P.G., Rennard, S.I., Foidart, J.M., and Martin, G.R. Laminin--a glycoprotein from basement membranes. J Biol Chem **254**, 9933, 1979.

29. Itoh, M., Nelson, C.M., Myers, C.A., and Bissell, M.J. Rap1 integrates tissue polarity, lumen formation, and tumorigenic potential in human breast epithelial cells. Cancer Res **67**, 4759, 2007.

30. Park, C.C., Zhang, H., Pallavicini, M., Gray, J.W., Baehner, F., Park, C.J., and Bissell, M.J. Beta1 integrin inhibitory antibody induces apoptosis of breast cancer cells, inhibits growth, and distinguishes malignant from normal phenotype in three dimensional cultures and in vivo. Cancer Res **66**, 1526, 2006.

31. Wang, F., Hansen, R.K., Radisky, D., Yoneda, T., Barcellos-Hoff, M.H., Petersen, O.W., Turley, E.A., and Bissell, M.J. Phenotypic reversion or death of cancer cells by altering signaling pathways in three-dimensional contexts. J Natl Cancer Inst **94**, 1494, 2002.

32. Weaver, V.M., Petersen, O.W., Wang, F., Larabell, C.A., Briand, P., Damsky, C., and Bissell, M.J. Reversion of the malignant phenotype of human breast cells in three-dimensional culture and in vivo by integrin blocking antibodies. J Cell Biol **137**, 231, 1997.

33. Sandal, T., Valyi-Nagy, K., Spencer, V.A., Folberg, R., Bissell, M.J., and Maniotis, A.J. Epigenetic reversion of breast carcinoma phenotype is accompanied by changes in DNA sequestration as measured by AluI restriction enzyme. Am J Pathol **170**, 1739, 2007.

34. Liu, H., Radisky, D.C., Wang, F., and Bissell, M.J. Polarity and proliferation are controlled by distinct signaling pathways downstream of PI3-kinase in breast epithelial tumor cells. J Cell Biol **164**, 603, 2004.

35. Isakoff, S.J., Engelman, J.A., Irie, H.Y., Luo, J., Brachmann, S.M., Pearline, R.V., Cantley, L.C., and Brugge, J.S. Breast cancer-associated PIK3CA mutations are oncogenic in mammary epithelial cells. Cancer Res **65**, 10992, 2005.

36. Muthuswamy, S.K., Li, D., Lelievre, S., Bissell, M.J., and Brugge, J.S. ErbB2, but not ErbB1, reinitiates proliferation and induces luminal repopulation in epithelial acini. Nat Cell Biol **3**, 785, 2001.

37. Yanochko, G.M. and Eckhart, W. Type I insulin-like growth factor receptor over-expression induces proliferation and anti-apoptotic signaling in a three-dimensional culture model of breast epithelial cells. Breast Cancer Res **8**, R18, 2006.

38. Weaver, V.M., Lelievre, S., Lakins, J.N., Chrenek, M.A., Jones, J.C., Giancotti, F., Werb, Z., and Bissell, M.J. beta4 integrin-dependent formation of polarized three-dimensional architecture confers resistance to apoptosis in normal and malignant mammary epithelium. Cancer Cell **2**, 205, 2002.

39. Bello-DeOcampo, D., Kleinman, H.K., Deocampo, N.D., and Webber, M.M. Laminin-1 and alpha6beta1 integrin regulate acinar morphogenesis of normal and malignant human prostate epithelial cells. Prostate **46**, 142, 2001.

40. Wang, F., Weaver, V.M., Petersen, O.W., Larabell, C.A., Dedhar, S., Briand, P., Lupu, R., and Bissell, M.J. Reciprocal interactions between beta1-integrin and epidermal growth factor receptor in three-dimensional basement membrane breast cultures: a different perspective in epithelial biology. Proc Natl Acad Sci U S A **95**, 14821, 1998.

41. Debnath, J., Mills, K.R., Collins, N.L., Reginato, M.J., Muthuswamy, S.K., and Brugge, J.S. The role of apoptosis in creating and maintaining luminal space within normal and oncogene-expressing mammary acini. Cell **111**, 29, 2002.

42. Kirshner, J., Chen, C.J., Liu, P., Huang, J., and Shively, J.E. CEACAM1-4S, a cell-cell adhesion molecule, mediates apoptosis and reverts mammary carcinoma cells to a normal morphogenic phenotype in a 3D culture. Proc Natl Acad Sci U S A **100**, 521, 2003.

43. Simian, M., Hirai, Y., Navre, M., Werb, Z., Lochter, A., and Bissell, M.J. The interplay of matrix metalloproteinases, morphogens and growth factors is necessary for branching of mammary epithelial cells. Development **128**, 3117, 2001.

44. Clejan, S., O'Connor, K., and Rosensweig, N. Tri-dimensional prostate cell cultures in simulated microgravity and induced changes in lipid second messengers and signal transduction. J Cell Mol Med **5**, 60, 2001.

45. Sun, S.Y., Rosenberg, L.M., Wang, X., Zhou, Z., Yue, P., Fu, H., and Khuri, F.R. Activation of Akt and eIF4E survival pathways by rapamycin-mediated mammalian target of rapamycin inhibition. Cancer Res **65**, 7052, 2005.

46. Sabers, C.J., Martin, M.M., Brunn, G.J., Williams, J.M., Dumont, F.J., Wiederrecht, G., and Abraham, R.T. Isolation of a protein target of the FKBP12-rapamycin complex in mammalian cells. J Biol Chem **270**, 815, 1995.

47. Neef, M., Ledermann, M., Saegesser, H., Schneider, V., and Reichen, J. Low-dose oral rapamycin treatment reduces fibrogenesis, improves liver function, and prolongs survival in rats with established liver cirrhosis. J Hepatol **45**, 786, 2006.

48. Bjornsti, M.A. and Houghton, P.J. The TOR pathway: a target for cancer therapy. Nat Rev Cancer **4**, 335, 2004.

49. Debnath, J., Walker, S.J., and Brugge, J.S. Akt activation disrupts mammary acinar architecture and enhances proliferation in an mTOR-dependent manner. J Cell Biol **163**, 315, 2003.

50. Liu, X., Shi, Y., Han, E.K., Chen, Z., Rosenberg, S.H., Giranda, V.L., Luo, Y., and Ng, S.C. Downregulation of Akt1 inhibits anchorage-independent cell growth and induces apoptosis in cancer cells. Neoplasia **3**, 278, 2001.

51. Chan, S. Targeting the mammalian target of rapamycin (mTOR): a new approach to treating cancer. Br J Cancer **91**, 1420, 2004.

52. Vignot, S., Faivre, S., Aguirre, D., and Raymond, E. mTOR-targeted therapy of cancer with rapamycin derivatives. Ann Oncol **16**, 525, 2005.

53. Steelman, L.S., Stadelman, K.M., Chappell, W.H., Horn, S., Basecke, J., Cervello, M., Nicoletti, F., Libra, M., Stivala, F., Martelli, A.M., and McCubrey, J.A. Akt as a therapeutic target in cancer. Expert Opin Ther Targets **12**, 1139, 2008.

54. Heinonen, H., Nieminen, A., Saarela, M., Kallioniemi, A., Klefstrom, J., Hautaniemi, S., and Monni, O. Deciphering downstream gene targets of PI3K/mTOR/p70S6K pathway in breast cancer. BMC Genomics **9**, 348, 2008.

55. Wendel, H.G., Malina, A., Zhao, Z., Zender, L., Kogan, S.C., Cordon-Cardo, C., Pelletier, J., and Lowe, S.W. Determinants of sensitivity and resistance to rapamycin-chemotherapy drug combinations in vivo. Cancer Res **66**, 7639, 2006.

56. Grunwald, V., DeGraffenried, L., Russel, D., Friedrichs, W.E., Ray, R.B., and Hidalgo, M. Inhibitors of mTOR reverse doxorubicin resistance conferred by PTEN status in prostate cancer cells. Cancer Res **62**, 6141, 2002.

57. Wendel, H.G., De Stanchina, E., Fridman, J.S., Malina, A., Ray, S., Kogan, S., Cordon-Cardo, C., Pelletier, J., and Lowe, S.W. Survival signalling by Akt and eIF4E in oncogenesis and cancer therapy. Nature **428**, 332, 2004.

58. Roudier, E., Mistafa, O., and Stenius, U. Statins induce mammalian target of rapamycin (mTOR)-mediated inhibition of Akt signaling and sensitize p53-deficient cells to cytostatic drugs. Mol Cancer Ther **5**, 2706, 2006.

59. Naoum, J.J., Woodside, K.J., Zhang, S., Rychahou, P.G., and Hunter, G.C. Effects of rapamycin on the arterial inflammatory response in atherosclerotic plaques in Apo-E knockout mice. Transplant Proc **37**, 1880, 2005.

60. Kawabata, K., Murakami, A., and Ohigashi, H. Citrus auraptene targets translation of MMP-7 (matrilysin) via ERK1/2-dependent and mTOR-independent mechanism. FEBS Lett **580**, 5288, 2006.

61. Lawrence, D.M., Singh, R.S., Franklin, D.P., Carey, D.J., and Elmore, J.R. Rapamycin suppresses experimental aortic aneurysm growth. J Vasc Surg **40**, 334, 2004.

62. Heimberger, A.B., Wang, E., McGary, E.C., Hess, K.R., Henry, V.K., Shono, T., Cohen, Z., Gumin, J., Sawaya, R., Conrad, C.A., and Lang, F.F. Mechanisms of action of rapamycin in gliomas. Neuro Oncol **7**, 1, 2005.

63. Eshleman, J.S., Carlson, B.L., Mladek, A.C., Kastner, B.D., Shide, K.L., and Sarkaria, J.N. Inhibition of the mammalian target of rapamycin sensitizes U87 xenografts to fractionated radiation therapy. Cancer Res **62**, 7291, 2002.

64. Guba, M., von Breitenbuch, P., Steinbauer, M., Koehl, G., Flegel, S., Hornung, M., Bruns, C.J., Zuelke, C., Farkas, S., Anthuber, M., Jauch, K.W., and Geissler, E.K. Rapamycin inhibits primary and metastatic tumor growth by antiangiogenesis: involvement of vascular endothelial growth factor. Nat Med **8**, 128, 2002.

65. Avellino, R., Romano, S., Parasole, R., Bisogni, R., Lamberti, A., Poggi, V., Venuta, S., and Romano, M.F. Rapamycin stimulates apoptosis of childhood acute lymphoblastic leukemia cells. Blood **106**, 1400, 2005.

66. Ghayad, S.E., Bieche, I., Vendrell, J.A., Keime, C., Lidereau, R., Dumontet, C., and Cohen, P.A. mTOR inhibition reverses acquired endocrine therapy resistance of breast cancer cells at the cell proliferation and gene-expression levels. Cancer Sci **99**, 1992, 2008.

67. Hay, N. The Akt-mTOR tango and its relevance to cancer. Cancer Cell **8**, 179, 2005.

68. Lee, G.Y., Kenny, P.A., Lee, E.H., and Bissell, M.J. Three-dimensional culture models of normal and malignant breast epithelial cells. Nat Methods **4**, 359, 2007.

69. Debnath, J., Muthuswamy, S.K., and Brugge, J.S. Morphogenesis and oncogenesis of MCF-10A mammary epithelial acini grown in three-dimensional basement membrane cultures. Methods **30**, 256, 2003.

70. Huss, F.R. and Kratz, G. Mammary epithelial cell and adipocyte co-culture in a 3-D matrix: the first step towards tissue-engineered human breast tissue. Cells Tissues Organs **169**, 361, 2001.

71. Gadducci, A., Cosio, S., and Genazzani, A.R. Old and new perspectives in the pharmacological treatment of advanced or recurrent endometrial cancer: hormonal therapy, chemotherapy and molecularly targeted therapies. Crit Rev Oncol Hematol **58**, 242, 2006.

72. Figlin, R.A., Brown, E., Armstrong, A.J., Akerley, W., Benson, A.B., 3rd, Burstein, H.J., Ettinger, D.S., Febbo, P.G., Fury, M.G., Hudes, G.R., Kies, M.S., Kwak, E.L., Morgan, R.J., Jr., Mortimer, J., Reckamp, K., Venook, A.P., Worden, F., and Yen, Y. NCCN Task Force Report: mTOR inhibition in solid tumors. J Natl Compr Canc Netw **6 Suppl 5**, S1, 2008.

73. Sawyers, C.L. Will mTOR inhibitors make it as cancer drugs? Cancer Cell **4**, 343, 2003.

74. Pieretti-Vanmarcke, R., Donahoe, P.K., Pearsall, L.A., Dinulescu, D.M., Connolly, D.C., Halpern, E.F., Seiden, M.V., and MacLaughlin, D.T. Mullerian Inhibiting Substance enhances subclinical doses of chemotherapeutic agents to inhibit human and mouse ovarian cancer. Proc Natl Acad Sci U S A **103**, 17426, 2006.

75. Mondesire, W.H., Jian, W., Zhang, H., Ensor, J., Hung, M.C., Mills, G.B., and Meric-Bernstam, F. Targeting mammalian target of rapamycin synergistically enhances chemotherapy-induced cytotoxicity in breast cancer cells. Clin Cancer Res **10**, 7031, 2004.

76. Johnson, K.R., Leight, J.L., and Weaver, V.M. Demystifying the effects of a three-dimensional microenvironment in tissue morphogenesis. Methods Cell Biol **83**, 547, 2007.

77. Moore, M.M., Whitney, L.A., Cerilli, L., Imbrie, J.Z., Bunch, M., Simpson, V.B., and Hanks, J.B. Intraoperative ultrasound is associated with clear lumpectomy margins for palpable infiltrating ductal breast cancer. Ann Surg **233**, 761, 2001.

78. Rejniak, A.K. A single cell-based model of the ductal tumour microarchitecture. Computational and Mathematical Methods in Medicine **8**, 61, 2007.

79. Doyle, T.E., Warnick, K.H., and Carruth, B.L. Histology-based simulations for the ultrasonic detection of microscopic cancer in vivo. J Acoust Soc Am **122**, EL210, 2007.

80. Taggart, L.R., Baddour, R.E., Giles, A., Czarnota, G.J., and Kolios, M.C. Ultrasonic characterization of whole cells and isolated nuclei. Ultrasound Med Biol **33**, 389, 2007.

81. Hunt, J.W., Worthington, A.E., Xuan, A., Kolios, M.C., Czarnota, G.J., and Sherar, M.D. A model based upon pseudo regular spacing of cells combined with the randomisation of the nuclei can explain the significant changes in high-frequency ultrasound signals during apoptosis. Ultrasound Med Biol **28**, 217, 2002.

82. Doyle, T.E., Robinson, D.A., Jones, S.B., Warnick, K.H., and Carruth, B.L. Modeling the permittivity of two-phase media containing monodisperse spheres: Effects of microstructure and multiple scattering. Phys Rev B **76**, 054203, 2007.

APPENDICES

APPENDIX A

LABORATORY PROTOCOLS

MAINTENANCE OF BREAST CANCER CELL LINES

I recommend adding 10 mL of Pen-Strep & 1 mL of Fungizone to every 500 mL of Media

CRL-8799 (or 184B5)

- Non-cancer epithelial cell line, **21**-year-old female
- Cells reach confluence in 3-5 days, growth spreads very rapidly
- **Media**: Use Mammary Epithelial Growth Medium (MEGM) from Clonetics.
    - Comes in a kit with MEBM & a series of supplements.
    - Do *not* add gentamycin-amphotericin B for CRL-8799 cells.
    - Save ¼ of the media, and exclude the EGF additive.
        - This media is to be used for 3D assays.
    - Also supplement all media with 1 ng/ml cholera toxin.
    - Serum Free
- Cytoprotectant media contains 10% FBS & 5% DMSO.
- Cell growth and size is considerably lower when other media type is used.
- Optimum Seeding Density: Standard or 1x10^4 cells/mL
- Resistant to Trypsin-EDTA; Might take up to 15 minutes to come off plastic without mechanical force.

HTB-132 (or MDA-MB-468)

- Mammary gland adenocarcinoma cells (epithelial) 51-year-old female
- Cells reach confluence in 3-5 days, grows very rapidly. Cells tend to stack and bud off into the media, so frequent washing is recommended.
- **Media**: Use Leibovitz's L-15 Medium.
    - Complete by adding 10% FBS
    - Save ¼ of the original media, and only add 2% FBS.
        - This media is to be used for 3D assays.
    - **Important**: Cells grown in L-15 Media MUST be incubated in pure air.
        - Using enhanced CO2 levels will reduce viability.
    - RPMI-1640 can be used if the previous note is impossible.
- Cytoprotectant media contains 10% FBS & 5% DMSO.
- Optimum Seeding Density: Standard or 1x10^4 cells/mL

HTB-121 (BT-483)

- Mammary gland ducatal carcinoma cells (epithelial) 23-year-old female
- Cells are very sensitive to pH, temperature & humidity – Take good care
- Cell growth is patchy and slow; will probably never reach confluence.
- **Media**: Use RPMI-1640 formulated with:
    - 2 mM L-glutamine
    - 10 mM HEPES
    - 1 mM sodium pyruvate

- 4.5 g/L glucose
- 1.5 g/L sodium bicarbonate
  - **Then, to prepare for culture supplement with:**
- 20% FBS
- 0.01 mg/ml bovine insulin
- Save ¼ of the original media, and only add 2% FBS.
  - This media is to be used for 3D assays.

- Cytoprotectant media contains 20% FBS & 5% DMSO.
- Optimum Seeding Density: High or 2.5x10^4 cells/mL

3D CULTURE PROCEDURE (on-top protocol)

1. Thaw the BME overnight at 4°C.
   a. Aliquot if many freeze-thaws are to be conducted.
   b. Keep the BME tube on ice at ALL times.
2. Pre-chill the plate(s) or dish(es) to be used in a freezer.
3. Make the assay media by mixing **cold** media with BME (EHS) to between 2 and 10%. Lower concentration promotes more growth & vice versa.
   a. Also, lower concentrations of FBS (2-5%) may be desirable.
4. Follow **Table 3** below for Gel Coat & Medium volumes.

Table 3: Recommended Gel Culture Parameters

If the well area listed in the table is different from the wells you are using, volumes should be adjusted. [68]

Type	# of Wells	Diameter (mm)	Area (cm^2)	Media Volume (µL)	EHS coat (µL)
Dish		60	28.3	5,000	850
Plates	6	35	9.6	2,000	500
	24	16	2	500	120
	48	10	0.75	200	80
	96	6	0.26	60	15

5. Coat the wells with the EHS coat volume and spread evenly with pipette tip.
    a. Be careful to avoid bubbles – it will dry that way.
    b. Due to the meniscus effect, there may be a bare spot in the center. If this is a problem, use a little extra gel.
6. Let the gels set for 15-20 minutes at 37°C.
7. Prepare the cells to be plated by diluting to the Medium volume in assay medium. (following the table above)
    a. A good seeding density to start with is 0.2x10^5 cells/cm^2 and 0.25x10^5 cells/cm^2 for malignant and normal cells.
8. Pipette evenly over the gels & incubate at 37°C.
9. Change assay media every 2 days.

3D EXTRACTION PROCEDURE (on-top protocol)

This protocol is for extraction of colonies from the gels without disrupting the cells themselves.

1. Make a stock solution of PBS-EDTA:
    a. 5 mM EDTA, 1 mM NaVO4, 1.5 mM NaF in PBS
2. Prepare Ice cold PBS & PBS-EDTA
3. Aspirate the media and rinse with ice-cold PBS 2 times.
    a. Note that all steps need to be done at 2-8°C.
4. Add 2-3 media volumes of PBS-EDTA.
5. Gently detach the gel by scraping with a pipette tip.
6. Shake gently for 15-30 min.
    a. If in-well imaging is the desired endpoint you can stop here, allow the cells to settle to the bottom and fix.
7. Transfer the contents to a tube, and rinse the wells with 0.5 media volume and transfer the rinse to the tube. Shake the tube (on ice) for 15-30 min.
    a. If transferring colonies to slides for imaging, centrifuge at minimum speed for 1-2 minutes, and carefully pipette 20 µl of colonies to slide.
    b. For protein or RNA extraction, additional washing with PBS-EDTA and re-centrifugation and re-suspension will reduce contaminating BME.

IMMUNOSTAINING PROCEDURE

Reference these 2 papers: [68, 69] These steps are for 96-wells or slides.

Reagents

- PBS Glycine: 100 mM Glycine in PBS
- IF Buffer: 0.2 % Triton, 0.1% BSA, 0.05% Tween 20 in PBS, 7.7 mM NaN3
- IF Block: 10% Goat Serum, 1% goat F(ab') IgG in IF Buffer

1. Fixation method depends on the antibody. This may include Formalin (Room Temp), Paraformaldehyde (RT), or 50/50 Methanol/Acetone (-20°C).
    a. I've had good results with 4% Paraformaldehyde for 15 minutes.
2. Rinse with PBS-Glycine 3x for 10 minutes.
3. Incubate in 100 µl of IF Block for 1.5 hours (use Parafilm for slides)
4. Stain with Primary antibody in 100 µl of IF Buffer for 2 hours or overnight at 2-8°C. Check product info for recommended concentrations of antibody.
5. Wash 3x for 20 min in IF Buffer.
6. Stain with Secondary antibody in 100 µl of IF Buffer for 45 minutes.
7. Wash for 20 min with IF Buffer.
8. Wash 2x for 10 min in PBS.
9. Counterstain Nuclei with DAPI or Ethidium Bromide for 5 minutes.
10. Wash with PBS for 10 minutes.
11. Observe and troubleshoot if needed.

RT PCR PROTOCOL (using SABiosciences PCR Arrays)

RNA Extraction (using QIAGEN RNeasy kit)

1. Sterilize all workspace and instruments by wiping down with RNase-away.
2. Acquire cell pellet in a centrifuge tube, and remove its supernatant.
3. Add 1 volume of Buffer RLT, and vortex the pellet.
    a. For <5x10^6 cells use 350 ul, otherwise, use 600 ul
4. Continue vortexing continuously for 1 minute.
5. Add 1 volume of 70% ethanol and mix well by pipetting.
    a. Remember to use ONLY RNase-free water.
6. Transfer to an RNeasy spin column and centrifuge for 15 s at 8000 g (max speed)
7. OPTIONAL DNase step
    a. Add 350 ul Buffer RW1 and spin for 15 s at max speed.
    b. In a separate tube, add 10 ul about 30 ku/ul DNase stock to 70 ul Buffer RDD
    c. Add all 80 ul to column and incubate at RT for 15 min
    d. Add 350 ul Buffer RW1 and spin at max speed.
8. Add 700 ul Buffer RW1 and spin 15 s at max speed.
9. Add 500 ul Buffer RPE and spin 15 s at max speed.
10. Add 500 ul Beffer RPE and spin 2 min at max speed.
11. Switch to new collection tube and spin for 1 min at max speed.
12. Switch column to final collection tube for elution.
13. Add 30-50 ul RNase-free water and spin for 1 min at max speed.

14. OPTIONAL: repaeat step 13 to increase yield of eluted RNA.

15. RNA can be stored at -80 C.

RNA Analysis

1. First **quantify** RNA conc. By measuring A260.
    - **a.** Remember to Blank.
    - **b.** Use conversion of 1 = 44 ug / ml
    - **c.** Concentration should be greater than 4 ug / ml
2. Check **Purity** by measuring 260/280 ratio.
    - **a.** 2.0-2.1 is a good ratio. (must be >2.0)
    - **b.** Also be sure the 260/230 ratio is >1.7
3. Prepare a Nano LabChip for use with an Agilent BioAnalyzer.
    - **a.** Prepare 1 ul samples of 30 ng/ul RNA.
    - **b.** 18S & 28S peaks should be sharp without shoulders or smears.
    - **c.** Alternately, a gel could be run to do this check.

cDNA Synthesis

1. Prepare DNA Elimination Mixture by adding 2 ul 5X gDNA Elimination Buffer to Total RNA, diluting to a total volume of 10 ul with RNase-free water.
    a. Total RNA range must be between 25 ng & 5 ug.
    b. Use same amount of RNA for each sample.
    c. The higher the amount the better for accuracy.
2. Prepare the RT Cocktail for all samples using **Table 4**.

Table 4: Reverse Transcriptase Recipe

RT Cocktail	**1 reaction**	**2 reactions**	**4 reactions**
BC3 (5X RT Buffer 3)	**4 ul**	**8 ul**	**16 ul**
P2 (Primer & External Control Mix)	**1 ul**	**2 ul**	**4 ul**
RE3 (RT Enzyme Mix 3)	**3 ul**	**6 ul**	**12 ul**
Final Volume	**10 ul**	**20 ul**	**40 ul**

3. **cDNA Synthesis Reaction:**
    a. Add 10 ul of RT Cocktail to each 10 ul DNA Elimination Mixture & mix well with pipette.
    b. Incubate at 42 C for **exactly** 15 min and **immediately** stop reaction by heating at 95 C for 5 minutes.
    c. Add 91 ul of ddH20 to each 20 ul reaction tube, mix well.
4. **OPTIONAL:** Set aside 6 ul of the cDNA template for RNA Quality Control Check.
5. Store template at -20 C until use.

RT PCR STEP

1. Mix the following in a separate tube to a total Volume of 2550 ul:
    a. 1275 ul 2X SABiosciences RT2 qPCR Master Mix
    b. 102 ul Diluted First Strand cDNA Syntehsis Reaction
    c. 1173 ul ddH2O
2. Add 25 ul of Experimental cocktail to each well of the Array Plate
3. Tightly Seal the plates with the provided 8-cap strips.
    a. Tap out any bubbles that may exist in the wells.
    b. Place on ice will setting up cycling program
4. Use **Table** 5 to set up and run the program

Table 5: RT-PCR Program

Cycles	Duration	Temperature
1	**10 minutes**	**95 C**
40	**15 seconds**	**95 C**
	30 – 40 seconds	**55 C**
	30 seconds	**72 C**

5. Use the instrument's software to approximate the threshold cycle
    a. Use the readings from cycle 2 through 2 cycle values before the earliest visible amplication (between 10 and 15) to set the baseline.
    b. Use Log View of the amp. Plots and place the threshold value within the lower one-third to lower one-half of the linear phase.
    c. Be sure the thresholds are the same across all PCR array runs. The value of CtPPC should be 18-22 across all arrays.
    d. Export the values for analysis.
6. Run a Dissociation (Melting) Curve
    a. Use the instrument's default, or run the following program:
    b. 95 C, 1 min; 65 C, 2 min (OPTICS OFF); 65 C to 95 C at 2 C / min (OPTICS ON)
7. Visually inspect the plate for any evaporation, noting specific wells.
8. Go to http://www.SABiosciences.com/pcrarraydataanalysis.php

APPENDIX B

RAW DATA

Table 6: Caspase Data for Malignant Cells

Caspase Activity for BT-483 Cells					
Values are in RLUs					
	Control	5 nm 24 hr	5 nm 48 hr	20 nm 24 hr	20 nm 48 hr
Sample	7181	18080	14372	19621	24089
	7321	11994	14468	23288	24676
Avg.	7251	15037	14420	21455	24383
St. Dev	3200	4303	68	2593	415

Table 7: Caspase Data for Normal Cells

Caspase Activity for 184-B5 Cells					
Values are in RLUs					
	Control	5 nm 24 hr	5 nm 48 hr	20 nm 24 hr	20 nm 48 hr
Sample	79597	78263	75927	69469	271317
	61911	66786	74365	54926	458742
Avg.	70754	72524	75146	62197	365029
St. Dev	12506	8115	1105	10283	132529

Table 8: Proliferation Data for Day 3

Values are in RFUs				
184B5 Ctrl	184B5 Rap	MDA-MB-468 Ctrl	MDA-MB-468 Rap	Blank
7942	6654	28022	24336	14
7756	7396	28492	25026	-85
8372	7746	29419	24271	71
8023.33333	7265.333	28644.33	24544.33	avg
315.951473	557.6032	710.849	418.3997	stdev

Table 9: Proliferation Data for Day 7

Values are in RFUs				
184B5 Ctrl	184B5 Rap	MDA-MB-468 Ctrl	MDA-MB-468 Rap	Blank
6135	5205	31703	16569	155
8362	5840	40376	22460	-214
7535	5626	37569	19386	58
7344	5557	36549.33	19471.67	avg
1125.71888	323.0743	4425.497	2946.434	stdev

Table 10: Cutoff RT-PCR Fold Change Values

Gene Category	Symbol	Description	Fold Change
Basement Membrane Constituents	COL7A1	Collagen, type VII, alpha 1	3.11
Cell-Cell Adhesion	ICAM1	Intercellular adhesion molecule 1	4.20
Cell-Matrix Adhesion	ITGA1	Integrin, alpha 1	1.54
	ITGA3	Integrin, alpha 3	2.80
	ITGA5	Integrin, alpha 5	1.28
	ITGB4	Integrin, beta 4	3.10
	SPP1	Secreted phosphoprotein 1	2.53
Collagens & ECM Structural Constituents	COL16A1	Collagen, type XVI, alpha 1	1.02
ECM Protease Inhibitors	TIMP1	TIMP metallopeptidase inhibitor 1	0.55
	TIMP2	TIMP metallopeptidase inhibitor 2	2.38
ECM Proteases	ADAMTS1	ADAM metallopeptidase	3.99
	MMP14	Matrix metallopeptidase 14	2.72
	SPG7	Spastic paraplegia 7	2.05
Other Adhesion Molecules	LAMB1	Laminin, beta 1	4.39
	THBS2	Thrombospondin 2	4.14
	TNC	Tenascin C	2.25
Other ECM Molecules	CTGF	Connective tissue growth factor	2.91
	ECM1	Extracellular matrix protein 1	1.48
	VTN	Vitronectin	0.69
Transmembrane Molecules	PECAM1	Platelet/endothelial cell adhesion molecule	3.73

Table 11: RT-PCR Quality Control

Quality Control Check (Ct values)						
	Avg RTC	Avg PPC	stdev RTC	stdev PPC	RTC - PCC	gDNA
Cntr. Plate	21.42	18.12	0.31	0.20	3.30	36.68
Exp.Plate	21.95	17.96	0.19	0.19	3.99	36.20

Table 12: Incalculable RT-PCR Data

Gene Category	Symbol	Description	CTL Ct	TRT ct	+/-
Basement Membrane Constituents	LAMA1	Laminin, alpha 1	N	31.3	+
Cell-Matrix Adhesion	ADAMTS8	ADAM metallopeptidase	N	34.98	+
	ITGA8	Integrin, alpha 8	34.19	N	-
	ITGAM	Integrin, alpha M	N	34.36	+
Collagens & ECM Structural Constituents	COL6A1	Collagen, type VI, alpha 1	N	30.88	+
ECM Proteases	MMP11	Matrix metallopeptidase 11	N	32.53	+
	MMP16	Matrix metallopeptidase 16	N	34.48	+
	MMP3	Matrix metallopeptidase 3	N	32.07	+
	MMP7	Matrix metallopeptidase 7	32.91	N	-
	MMP9	Matrix metallopeptidase 9	N	33.03	+
Other Adhesion Molecules	CNTN1	Contactin 1	N	34.37	+
	COL15A1	Collagen, type XV, alpha 1	30.27	N	-
	KAL1	Kallmann syndrome 1 sequence	N	34.75	+
Other ECM Molecules	HAS1	Hyaluronan synthase 1	N	34.04	+
	THBS3	Thrombospondin 3	N	31.958	+
Transmembrane Molecules	SELL	Selectin L	N	33.211	+
	VCAM1	Vascular cell adhesion molecule 1	N	34.066	+

Table 13: Complete List of Cell Colony Areas

Units in (μm)^2					
184-B5		**BT-483**		**MDA-MB-468**	
w/ EGF	**w/o EGF**	**w/o RAP**	**w/ RAP**	**w/o RAP**	**w/ RAP**
5119	37500	68004	3563	39203	2540
4711	24880	44360	3472	15722	886
4419	12171	37724	3208	11708	2324
4393	15792	22652	2927	11243	2553
4299	6583	21969	2798	18713	1505
4241	6506	16455	2667	6688	1388
4013	10215	13987	2349	4963	3070
3618	6636	12208	2307	29354	2733
3574	11789	11883	2188	10439	3000
3374	13017	10643	2062	18998	1571
3346	8903	10403	2039	26904	2596
3137	7489	8335	2014	10612	2607
2946	3384	11986	2004	18212	1475
2929	15598	30362	1980	26758	2299
2855	13828	28154	1944	27729	3737
2765	42713	17008	1930		1071
2593	38484	11814	1864		968
2581	28947	6139	1790		1063
2548	28770	7615	1738		2004
2499	28715		1728		3074
2386	20680		1711		2307
2379			1664		2259
2362			1640		2385
2272			1579		3186
2236			1570		1038
2060			1523		1448
1929			1501		1214
1820			1404		922
1712			1350		
1600			1340		
1543			1315		
1101			1286		
2075			1277		
3116			1165		

4367			1155		
4231			1144		
4004			1114		
3991			1083		
3886			1041		
3626			984		
3483			959		
3304			950		
2838			938		
2803			897		
2734			812		
1894			603		
1705			3149		
1562			754		
3105			654		
2761			1008		
2748			568		
2352			817		
2080			545		
2016			1834		
1967			1087		
1714			1721		
1618			1376		
1536					
546					
513					
1051					
2400					
1120					
1983					
1290					
1362					
1490					